To the Graduate Council:

I am submitting herewith a thesis written by Corinne Grady Ciaccio entitled "Bifunctional Interpenetrating Polymer Networks: Synthesis and Investigation of the Microenvironmental Effect." I have examined the final copy of this thesis for form and content and recommend that it be accepted in partial fulfillment of the requirements for the degree of Master of Science, with a major in Chemistry.

Spiro D. Alexandratos, Major Professor

We have read this thesis
and recommend its acceptance:

Accepted for the Council:

Associate Vice Chancellor
and Dean of The Graduate School

BIFUNCTIONAL INTERPENETRATING POLYMER NETWORKS: SYNTHESIS AND INVESTIGATION OF THE MICROENVIRONMENTAL EFFECT

A Thesis

Presented for the

Master of Science

Degree

The University of Tennessee, Knoxville

Corinne Grady Ciaccio

December 1992

To my husband Jay and to my family

ACKNOWLEDGEMENTS

I am grateful to Professor Spiro D. Alexandratos for his excellent direction and encouragement. I would like to thank Darrell, Frank, Andrezj, and David for their assistance in the laboratory. Also, I would like to acknowledge the support of the Millsaps College Chemistry Department during the writing of this work. Finally, I acknowledge the Department of Energy, Office of Basic Energy Sciences, for financial support.

ABSTRACT

Interpenetrating Polymer Networks (IPNs) consisting of polystyrene as network I and poly(vinyl imidazole-co-ethyl acrylate) as network II have been developed. The synthesis of the IPNs is sequential and utilizes a suspension polymerization procedure. The monomer feed ratios were varied so that definite ratios of the imidazole and ester ligands could be achieved. IPNs with the imidazole and carboxylic acid moiety were obtained after hydrolysis of the ester groups. These ligands are important since the imidazole has coordinating capabilities, while the carboxylic acid ion exchanges. Therefore, the IPNs are an outgrowth of a new category of polymers termed dual mechanism bifunctional polymers which contain two groups on the same support network each of which operates by a different mechanism.

The ester and carboxylic acid ligands also altered the microenvironment surrounding the coordinating imdazole. This microenvironmental effect was investigated with molecular and ionic recognition studies, and binding constants (K_{11}) were measured. Phenylphosphinic acid was the substrate utilized for the molecular studies and was contacted with imidazole-based IPNs. Molecular recognition studies were also completed with polymer-supported dimethylamine ligands as a companion study to the imidazole IPNs. These experiments utilized substituted benzoic acids and were analyzed with Hammett type relationships. The polarity of the microenvironment was varied with increasing ratios of ester ligands and the effect was quantitatively realized in the K_{11}'s. Ionic recognition studies examined the effect of the

microenvironment in the imidazole-acid and imidazole-ester IPNs. Again, a series of IPNs with different ratios of the two ligands were synthesized and contacted with Cu(II), Co(II), Ni(II), Zn(II), and Cd(II). The binding constants displayed the effect of the microenvironment and were explained in terms of hard-soft acid base theory.

TABLE OF CONTENTS

CHAPTER PAGE

I. INTRODUCTION 1

II. SYNTHESIS OF INTERPENETRATING POLYMER NETWORKS 13

Introduction 13

Initial Approaches to Synthesis of Poly(vinyl imidazole) 15

Optimizing the Synthesis of Interpenetrating Polymer Networks 16

Hydrolysis of Interpenetrating Polymer Networks 25

Characterization of Interpenetrating Polymer Networks 30

III. MOLECULAR RECOGNITION 36

Introduction 36

The Microenvironmental Effect of Vinyl Imidazole-Based Interpenetrating Polymer Networks 37

The Microenvironmental Effect of Dimethyl-amine Resins 44

The Hammett Equation in Molecular Recognition Studies 44

The Effect of Partial Functionalization 45

The Effect of Solvent on Partially Functionalized Resins 52

The Effect of Crosslink Level 54

Conclusions 59

IV. IONIC RECOGNITION 60

Introduction 60

Initial Ionic Recognition Studies 62

Ionic Recognition Studies with Polystyrene/poly(vinylimidazole-co-ethyl acrylate) IPNs 65

Ionic Recognition Studies with Hydrolyzed polstyrene/poly(vinylimidazole-co-ethyl acrylate) IPNs 71

Conclusions 77

V. EXPERIMENTAL PROCEDURES 78

Xerogel Polystyrene Synthesis 78

Dimethylamine Resin Synthesis 80

Interpenetrating Polymer Network Synthesis 80

Acid Hydrolysis 82

Base Hydrolysis 82

Determination of Percent Solids 82

Determination of Acid Capacity 83

Determination of Base Capacity 84

Determination of Total Anion-Exchange Capacity 84

Determination of Salt Splitting Anion Exchange Capacity 85

Molecular Recognition Studies 85

Ionic Recognition Studies 87

Determination of Purity of Metal Salts 88

Copper 88

Cobalt 88

Zinc 88

Nickel 89

Cadmium 89

LIST OF REFERENCES 90

APPENDIX 96

VITA 103

LIST OF TABLES

TABLE		PAGE
1.	Classification of Interpenetrating Polymer Networks.	7
2.	Comparison of Aqueous Phases.	17
3.	Comparisons of Initiator, Crosslinking Agent, and Procedure.	19
4.	Investigation of Monomer Solutions in Toluene.	21
5.	Examination of Vinyl Imidazole with Co-Monomers.	22
6.	Comparison of Aqueous Phases and Level of Crosslinking.	24
7.	Attempted Hydrolyses of MMA IPNs.	26
8.	Attempted Hydrolyses of VIm-MMA IPNs.	27
9.	Hydrolysis Procedures for Ethyl Acrylate IPNs.	29
10.	Swelling Ratios of VIm-EA IPNs in Methanol and 1,4-Dioxane.	39
11.	Binding Constants of VIm-EA IPNs and PPA.	42
12.	Binding Constants of 40% and 100% DMA Resins with Substituted ArCOOH.	49
13.	K_{11}'s of Imidazole-Based IPNs with Cu(II) and Co(II) after 24 Hour Contact.	64
14.	K_{11}'s of VIm-EA IPNs with Cu(II) and Co(II).	69
15.	K_{11}'s of VIm-AA IPNs with Metal Ions.	75

LIST OF FIGURES

FIGURE PAGE

1. Polystyrene/Poly(vinylimidazole-co-ethyl acrylate). 12
2. Hydrolyzed Polystyrene/Poly(vinylimidazole-co-ethyl acrylate). 12
3. Vinylimidazole. 14
4. Methyl Methacrylate. 14
5. Ethyl Acrylate. 14
6. Infrared Spectra of VIm IPN. 31
7. Infrared Spectra of EA IPN (3-068B), VIm-EA IPN (3-046), and VIm IPN (2-038). 32
8. Infrared Spectra of Hydrolyzed EA IPN (2-172), Hydrolyzed VIm-EA IPN (3-001), and VIm IPN (2-038). 34
9. Infrared Spectra of Hydrolyzed VIm-EA IPN (2-048) and VIm-EA IPN. 35
10. Adsorption Isotherms for VIm-EA IPNs with PPA. 41
11. *y*-Reciprocal Plots for VIm-EA IPNs with PPA. 41
12. Binding Curve for 40% DMA with Substituted ArCOOH. 47
13. *y*-Reciprocal Plot for 40% DMA with Substituted ArCOOH. 47
14. Binding Curve for 100% DMA with Substituted ArCOOH. 48
15. *y*-Reciprocal Plot for 100% DMA with Substituted ArCOOH. 48
16. Hammett Plot of 100% DMA. 51
17. Hammett Plot of 40% DMA. 51
18. Adsorption Isotherm of 40% DMA with Benzoic Acids in 1,4-Dioxane. 53

19. Adsorption Isotherm of 100% DMA with Benzoic Acids in 1,4-Dioxane. 53

20. Percent Complexed by DMA Resins of Substituted ArCOOH at R_i=1.0. 56

21. Percent Complexed by DMA Resins of Substituted ArCOOH at R_i=0.5. 57

22. Percent Complexed by DMA Resins of Substituted ArCOOH at R_i=0.1. 58

23. Adsorption Isotherms of IPNs with Cu(II). 63

24. *y*-Reciprocal Plot of IPNs with Cu(II). 63

25. Adsorption Isotherm of VIm-EA IPNs with Cu(II). 67

26. *y*-Reciprocal Plot of VIm-EA IPNs with Cu(II). 67

27. Adsorption Isotherm of VIm-EA IPNs with Co(II). 68

28. *y*-Reciprocal Plot of VIm-EA IPNs with Co(II). 68

29. Adsorption Isotherms of VIm-AA IPNs with Cu(II). 72

30. *y*-Reciprocal Plots of VIm-AA IPNs with Cu(II). 72

31. Adsorption Isotherms of VIm-AA IPNs with Co(II). 73

32. *y*-Reciprocal Plots of VIm-AA IPNs with Co(II). 73

33. Adsorption Isotherms of VIm-AA IPNs with Cd(II). 74

34. *y*-Reciprocal Plots of VIm-AA IPNs with Cd(II). 74

A1. VIm Complexation of PPA. 98

A2. Adsorption Isotherm of VIm IPN with PPA. 100

A3. *y*-Reciprocal Plot of VIm IPN with PPA. 102

CHAPTER I

INTRODUCTION

Polymer-supported reagents and catalysts play increasingly important roles in many areas of chemistry. The field of polymer-supported ion-exchangers began in 1935 when two English chemists, Adams and Holmes, developed a resin with cation and anion exchangers that had better properties than any of the previous products[1]. In 1959, Merrifield realized the need for a rapid, quantitative, automatic method for the synthesis of long chain peptides. He invented a peptide synthesis on polymer supports and was honored with the Nobel Prize in Chemistry in 1984 for his achievement[2]. Since these first discoveries of the advantages of polymer supports, there has been continuing growth in the area of immobilizing reagents onto polymeric supports.

Styrene-based polymers are the most widely used supports[3], but acrylic ester and inorganic supports are being examined. Suspension (or bead) polymerization is ideally suited for the preparation of beaded polymeric materials and is the subject of several articles[4-6]. A good description of their synthesis, characteristics, and functionalization is given by Sherrington and Hodge[7]. In this process, droplets containing a mixture of styrene, or the desired monomer, and initiator are suspended in

an aqueous solution containing stabilizers which prevent the agglomeration of the monomer droplets. The temperature is then raised to effect polymerization, producing the polymer in the form of spherical gel beads ranging from 1 micron to 2 millimeters in diameter[8]. By selecting appropriate conditions, microporous or macroporous beads can be obtained. The former are prepared by using low levels of crosslinking agent (2 wt% divinylbenzene) and no additives. When the product is dried, the polymer matrix collapses to give beads with very small pores. Macroporous polymers are usually prepared using relatively large amounts of crosslinking agent and additives called porogens or diluents (toluene, certain alcohols, or linear polymers). Macroporous polymers are relatively rigid, and when dried, the large pores remain[3]. Important characteristics of the beads include bead size, porosity, swelling behavior, mechanical and thermal properties, and distribution of crosslink density.

The primary attraction of polymer-supported reagents and catalysts is that after one has been used in a reaction the polymer-supported species can be easily separated from the low molecular weight species in solution. Reactants bound to linear polymers have also been used by dissolving the polymeric reactant in a reaction solvent. At the end of the reaction period, the polymer is usually selectively precipitated out, then filtered off[3]. Easy separation of polymer species has several advantages[9]:

1) It may be possible to avoid exposing the products to water or to avoid chromatographic separation.

2) Substantial excesses of reagent may be used to obtain high reaction yields without causing separation problems.

3) It may be possible to recycle the polymer-supported species.

4) It may be possible to automate the procedure.

5) It may be possible to carry out the reactions and the recycling process using a column.

Another attractive feature of polymer-bound species is the reduced toxicity and the odor of supported reagents compared with low molecular weight species.

In the 1970's there was an increase in the use of polymeric reagents in general organic synthesis[2], which has continued. Polymer-supported Wittig reactions were some of the first polymer-supported reactions to be studied[10]. Several polymer-bound reagents for the oxidation of alcohols and allylic and benzylic halides have been reported[11-13]. Reducing agents, nucleophilic reagents, acylating agents, ylids, phosphines, and organometallic reagents have been successfully bound and utilized on polymer supports[3].

Polymer supports with quaternary ammonium and phosphonium ions have been applied as active catalysts for reactions of anions with nonpolar organic compounds in triphase solid/liquid/liquid mixtures [2,3,14]. Poly(ethylene glycol) monomethyl ethers grafted to crosslinked polystyrene can be highly active triphase catalysts for the alkylations of nitriles and alcohols, dehydrohalogenations and for saponifications of esters[3].

While polymer-supported species have contributed significantly to organic synthesis, their most notable use is as supports for ion exchangers. The importance of ion exchange has been recognized since the 19th century when Thompson and Way rediscovered cation exchange in soils[8]. Clays, glauconites, zeolites, and humic acids

were identified as ion exchangers, and such materials were used in attempts in plant operations for water softening and other purposes[8]. As previously discussed, Adams and Holmes prepared the first ion-exchange resin by direct polycondensation of phenolsulfonic acid with formaldehyde[1]. The first successful ion-exchange polymer synthesized by vinyl polymerization was prepared by d'Alelio in 1944 with acrylic acid and ethylene dimethacrylate[15]. In 1962, Helfferich[8] defined ion exchangers as insoluble solid materials which carry cations or anions that may be exchanged for a stoichiometrically equivalent amount of other ions of the same sign when the ion exchanger is in contact with an elecrolyte solution. Ion-exchange polymers have been the subject of several monographs[16-20] and have been applied to a wide variety of industrial, domestic, governmental, and laboratory operations.

Water treatment, including softening and deionization, constitutes 75% of the United States ion-exchange resin consumption[18]. Ion-exchange softening processes utilize sodium-cycle cation resins in both domestic and industrial applications. Deionization removes dissolved ionic impurities from water by a two-step treatment with cation- and anion-exchange resins. The former exchanges hydrogen ions for cations in solution. The acidic effluent passes through a hydroxide anion-exchange column that replaces the anions in solution with hydroxide[18].

In addition to water treatment, these resins have been employed in numerous other fields. Ion-exchange resins play an important role in the purification of sugars, including decolorization, softening, waste recovery, ion exclusion, and reverse softening[18]. In pharmaceutical processing, use of weak cation-exchange resins was

instrumental in the successful production of streptomycin[17]. Weak acid resins are also used to recover and purify neomycin, gentamycin, vitamin B_{12}, and kanamycin[18]. Ion-exchange chromatography provides the sole analytical technique for monitoring trace contaminants (ppb or less) in condensate polishing[21]. The application of ion-exchange technology to hydrometallurgical practices involves the isolation, purification, and concentration of metals from aqueous media[18]. Recently, phosphinic acid resins have received attention as extractants for use in metal ion recovery[22,23]. Ion-exchange resins are applied in many areas of chemical processing including purification, metals recovery, synthesis and chemical conversion, and waste and pollution control[18].

Helfferich[24] introduced and Janauer[25] extended the concept of reactive ion exchange (RIEX) as a method to increase selectivity in the isolation, concentration, or removal of a targeted species from a complex mixture. RIEX is defined as any process in which the ion-exchange reaction is directly coupled with another chemical reaction such as reduction, precipitation, chelation, neutralization, ion complex formation, ligand exchange, etc. Alexandratos and coworkers developed this concept and introduced a new category of resins, termed dual mechanism bifunctional polymers (DMBP's), for the selective complexation and recovery of metal ions[26].

A DMBP operates with two different functional groups by two different mechanisms which are labeled the access mechanism and the recognition mechanism. The access mechanism which is provided by an ion-exchange group allows for metal ion entry into and mobility within the polymer network. The recognition mechanism allows for metal ion specificity through a group responsible for reduction,

coordination, or precipitation on the same polymer. The dual mechanism bifunctional polymers are divided into three classes. Class I: ion-exchange/redox resins[27]; class II: ion-exchange/coordination resins[28]; class III: ion-exchange/precipitation resins[29] have been synthesized, and their metal ion affinities have been examined.

With bifunctional polymers, the two different types of ligands can cooperate synergistically to yield a reagent with enhanced complexing abilities relative to the monofunctional polymers. However, designing a high yield synthesis which binds the ligands to the support in the desired ratios can be difficult to achieve. Interpenetrating polymer networks (IPNs) are an alternative to the covalent immobilization of ligands onto a polymer support for the preparation of well-defined bifunctional polymers[30].

An interpenetrating polymer network (IPN) can be defined as a combination of two polymers in network form, at least one of which is synthesized and/or crosslinked in the immediate presence of the other[31]. The first use of the term "interpenetrating polymer network" was by Millar in 1960[32]. He investigated polystyrene/polystyrene IPNs and the sulfonic resins derived from them. Most IPN research has focused on the topology[31], and this may be attributed to the fact that there are many different ways that an IPN can be prepared. Each procedure yields an IPN with a distinctive topology and unique properties.

The different categories of IPNs are shown in Table 1[33]. They are classified according to their polymerization and crosslinking. The sequential and simultaneous IPNs have been examined more than the other types of IPNs.

Table 1. Classification of Interpenetrating Polymer Networks.

CATEGORY	DEFINITION
sequential IPN (SIPN)	polymer I is swollen in monomer II, its crosslinking agent, and initiator, polymerizing II in situ
simultaneous IPN (SIN)	monomers I and II, and their respective crosslinking agents and initiators, are polymerized simultaneously by way of noninterfering modes
latex interpenetrating elastomeric network (IEN)	linear polymers I and II are mixed and both components are crosslinked simultaneously
semi-I IPN	sequential IPN in which polymer I is crosslinked and polymer II is linear
semi-II IPN	sequential IPN in which polymer I is linear and polymer II is crosslinked
pseudo-IPN	simultaneous IPN in which one polymer is crosslinked and the other linear

The sequential IPN begins with the synthesis of a crosslinked polymer I. With its crosslinking agent and initiator, monomer II is swollen into polymer I and polymerized in situ[31]. Simultaneous IPNs begin with a solution of monomers I and II and their respective crosslinking agents, which are then polymerized simultaneously by noninterfering modes, such as stepwise and chain polymerizations.

Current IPN research has focused on several different topics. The synthesis of poly[bis((methoxyethoxy)ethoxy) phosphazene]/polymethyl methacrylate[34], poly(carbonate-urethane)/polymethyl methacrylate[35], and polyurethane/polystyrene[36] IPNs have been described. A study of the kinetics and degree of polymerization of poly(vinyl chloride)/polymethacrylate IPN systems has been completed by Abu-Isa[37], and Acevedo[38] studied the thermal properties of semi-IPNs of maleimide end-capped oligoesters. Kolarz investigated the properties and structure of poly(methacrylic acid)/polystyrene IPNs in the dry[39] and swollen[40] state. The morphology of IPNs has been studied frequently with current research focusing on the systems of poly(2,6-dimethyl-1,4-phenylene oxide) and high molecular weight rubber[41], poly(ethyl acrylate)/poly(styrene-co-methyl methacrylate)[42], and poly(2,6-dimethyl-1,4-phenylene dioxide)/polydimethylsiloxane[43]. The mechanical properties of several IPN systems have also been examined including polyurethanes/poly(methyl methacrylate)[44], polyurethane/poly(methyl acrylate)[45], castor oil polyester/poly(methyl methacrylate)[46], and polyurethane/epoxy resin[47].

Because the varied synthetic techniques yield IPNs with different properties, many diverse applications exist for IPNs. Several major classes of materials are

readily identified: (1) tough and/or impact resistant plastics, (2) reinforced elastomers, (3) noise- and vibration-damping compounds, (4) vulcanized rubber/rubber blends, (5) electrical insulators, (6) transport-selective compositions, (7) coatings and adhesives, and (8) ion-exchange resins[31].

Pater[48] investigated a simultaneous semi-IPN of a thermoset and a thermoplastic to develop tough and microcracking resistant high temperature matrix resins for use in aircraft/aerospace structural components. Sheet-molding compounds prepared from unsaturated polyester resin and styrene are used in transportation, appliances, and electrical devices[33]. In most rubber/rubber blends, the polymers are mechanically blended together in the linear state, and subsequently crosslinked via sulfer vulcanization, which constitutes a specialized type of IPN[49]. Nearly three million metric tons of rubber are used annually in the United States with 64% of it going into automotive tires. IPN systems also been developed for versatile drug delivery systems [50,51] and for materials resistant to cellular adhesion that have biomedical applications[52].

The first report of anionic/cationic IPNs for ion-exchange resins was by Solt[53] who was issued a patent in 1955, five years before the term "interpenetrating polymer network" was coined. He reported a sequential IPN of poly(vinyl benzylchloride)/polystyrene that reacted with trimethylamine to give quaternary ammonium groups on network I and hot concentrated sulfuric acid, which introduced sulfonic acid groups on network II. Kolarz[54] synthesized and investigated the properties of some sequential IPNs formed from polystyrene-co-divinylbenzene beads

and methacrylic acid, which produced carboxylic acid cation exchangers. In another study, Trochimczuk[55] swelled polyethylene with styrene/divinylbenzene mixtures. The films were then treated with chloromethyl ether in the presence of a catalyst which prepares the IPNs for ion exchange reactions. It was found that the polyethylene serves to mechanically strengthen the final ion-exchange resin by providing mechanical support.

The concept of using a porous or macroreticular network I to provide mechanical strength to an ion exchange resin was advanced by Barrett and Clemens[56]. The team studied strong base and strong acid homo- and hetero-IPNs with one of the networks densely crosslinked and the other lightly crosslinked[56]. One advantage of this composition was that the densely crosslinked network provides mechanical strength, while the lightly crosslinked network swells greatly, providing rapid ion-exchange capability. Hatch[57] described amphoteric ion-exchange resins containing a weak acid and a weak base in IPN form. A crosslinked weak acid or weak base ion exchange resin in microbead form was prepared and suspended in a liquid mixture of monomers which could be converted to a crosslinked matrix polymer of opposite ion exchange type. The monomer mixture was then polymerized to form a matrix resin having the microbead particles embedded therein.

This research involves the synthesis and characterization of well-defined bifunctional ion exchange/coordination polymers with ethyl acrylate (as the ion exchange precursor or monomer) and N-vinylimidazole (as the coordination ligand) being the initial monomer pair. The polymers were obtained in the form of sequential

IPNs with xerogel[58] polystyrene as network I and ethyl acrylate and N-vinylimidazole as the monomers in network II. After formation of the second network, the ester groups were hydrolyzed to give the carboxylic acid derivatives. The imidazole ligand may be used in the "free" amine form (at a pH below 7) or in the protonated form (at a pH above 7)[59]. Thus, imidazole can act either as a proton acceptor or a proton donor, depending on its environment and is applicable in a wide range of pH values. Imidazole has many other interesting properties and has been studied in a variety of roles[60-64].

Ethyl acrylate and the hydrolyzed ethyl acrylate were employed as a means of altering the microenvironment around the imidazole group. For each IPN containing ethyl acrylate, the carboxylic acid derivative was also studied as shown in Figure 1 and Figure 2. These IPNs, with carboxylic acid as ion-exchange site and the imidazole capable of coordination, are an outgrowth of the dual mechanism bifunctional polymers class II: ion-exchange/coordination resins.

Chapter II of this thesis describes the synthesis and characterization of the IPNs. To investigate the microenvironment of the IPNs, molecular recognition studies were conducted on a series of IPNs with different ratios of the imidazole and ester ligands. This is discussed in Chapter III. In addition to the small molecules, metal ions were used as probes of the microenvironment of the imidazole-ester IPNs and in the imidazole-acid IPNs, and this is the basis of Chapter IV. In the molecular and ionic recognition studies, binding constants, K_{11}, which quantitatively describe the strength of the interaction between substrate and ligand are employed.

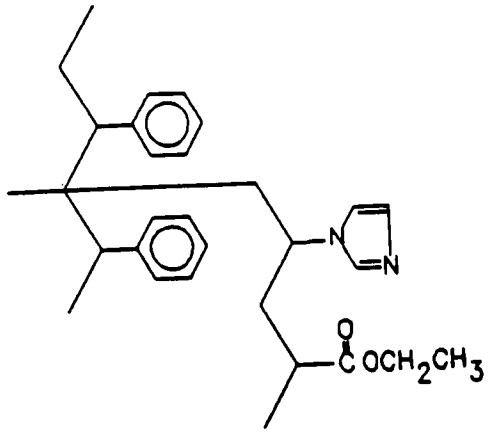


Figure 1. Polystyrene/poly(vinylimidazole-co-ethyl acrylate).

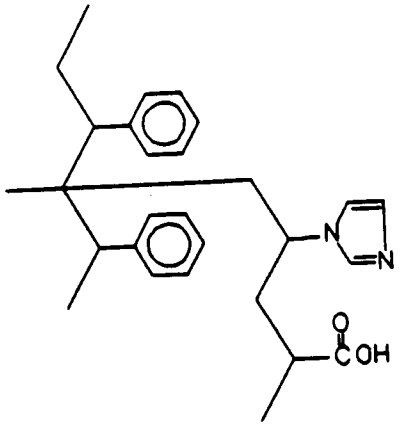


Figure 2. Hydrolyzed Polystyrene/poly(vinylimidazole-co-ethyl acrylate).

CHAPTER II

SYNTHESIS OF INTERPENETRATING POLYMER NETWORKS

Introduction

The method chosen to synthesize an interpenetrating polymer network or IPN determines the structure and the resulting properties of the polymer. As discussed earlier, several procedures and variables exist when working with IPNs, such as the choice of network I and II, the order and mode of polymerization, and if one or both networks is crosslinked. Also, the questions involved with the actual procedure are numerous, and they must be answered so that a maximum percent yield is achieved with both networks.

The first goal of the research was to synthesize a polymer containing vinylimidazole, and then synthesize a bifunctional polymer with definite ratios of the imidazole group for coordination and a carboxylic acid group for ion exchange. The monomers vinylimidazole (VIm), methyl methacrylate (MMA), and ethyl acrylate (EA) were employed and are shown in Figures 3-5. The functional groups must be

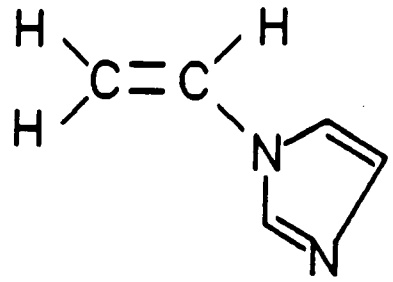


Figure 3. Vinylimidazole.

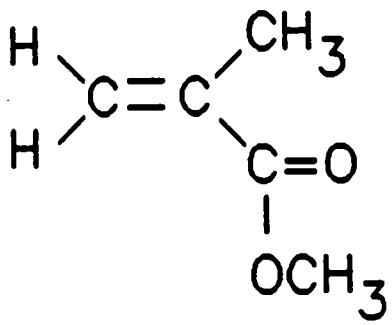


Figure 4. Methyl Methacrylate.

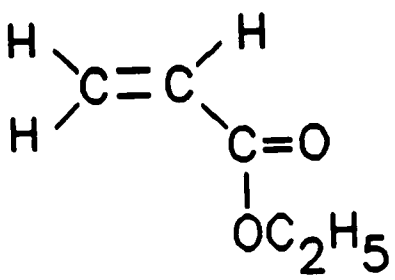


Figure 5. Ethyl Acrylate.

accessible for interaction with molecules and metal ions, and at the same time, the resin matrix must be crosslinked to give strength and stability to the polymer.

Initial Approaches to the Synthesis of Poly(vinyl imidazole)

Initial attempts to synthesize linear poly(vinyl imidazole) involved free-radical polymerizations similar to Dambatta and coworkers[64] and Bamford and Schofield[65]. Solutions consisting of vinylimidazole (VIm), initiator azobisisobutyronitrile (AIBN), and toluene were stirred and heated. Concentrations from 1 M to 4 M were examined and resulted in dark brown insoluble liquids. Solutions with both VIm and methacrylic acid (MAA) as monomers were investigated but yielded no useful polymer. Different solvents including ethanol, tetrahydrofuran, and benzene did not improve the product.

A crosslinking agent was then examined with the vinylimidazole in hopes that a more substantial product could be obtained. A 2 M solution of VIm and MAA with 20 mol % divinyl benzene (DVB) in ethanol was heated for 12 hours. A white powder was obtained. The crosslinking agent diethylene glycol diacrylate was also investigated and gave a white solid. Attempts to titrate or otherwise measure the capacity with a total anion-exchange capacity of the brown liquids or the white solids proved unsuccessful. Also, the products were difficult to use due to their physical properties (the white solid was a powder and the brown liquid was very viscous).

Placing the desired functional groups, imidazole and carboxylic acid, covalently onto a polymer support was not plausible, due to the fact that it would be difficult to synthesize a polymer with these two groups present in definite ratios.

Optimizing the Synthesis of Interpenetrating Polymer Networks

An important alternative to covalently binding a functional group to a support is to immobilize a polymer network within another polymer network. This sequential IPN synthesis allows the second network to form more easily and gives it more stability. Alexandratos and Strand[66] investigated IPNs that contained macroporous polystyrene as network I and diundecenyl phosphate as network II. For the vinylimidazole (VIm) based IPNs, xerogel[58] polystyrene beads were utilized as the support structure, network I. Polystyrene is compatible with a wide range of compounds having varying polarities and is synthesized on a large scale for many uses. The xerogel polystyrene is synthesized with 2 wt % DVB and 40 wt % toluene to give beads with larger micropores and good swelling capabilities.

The first IPNs were completed with the second network formed by suspension polymerization. Initially, two aqueous phases were examined. The first (IPN CG1-102) contained poly(diallydimethylammonium chloride) or PADMAC, gelatin, and boric acid in water. The PADMAC serves as a suspending agent and increases the viscosity of the aqueous phase, the gelatin is a stabilizer to keep the beads from agglomerating, and the boric acid acts as a buffer to keep the gelatin dissolved. The

second aqueous phase (IPN 1-121) was composed of the same amount of PADMAC and 1 g NaCl for every 3 mL of H_2O. The NaCl increased the ionic strength of the aqueous phase. The polystyrene beads were swelled with a monomer solution containing 18 mol% DVB, 1 wt % AIBN, and VIm. The beads were placed in the monomer solution 24 hours in order to ensure complete swelling. Next, the swollen beads were placed in the aqueous phase and were stirred and heated for 12 hours at 80 °C.

The results are shown in Table 2. The VIm capacity is always measured in units of milliequivalents per dry gram of polymer (meq/g). Vinyl imidazole is extremely water soluble and would leech out of the swollen beads into the aqueous phase before the polymerization was complete. Increasing the ionic strength with NaCl increased the percent yield 1.5 times more than the aqueous phase without the higher ionic strength. Therefore, the aqueous phase of 1-121 was used for the IPNs in the following experiments.

Table 2. Comparison of Aqueous Phases.

Resin	Aqueous Phase	Solids (%)	VIm Capacity	Yield (%)
CG1-102	PADMAC, gelatin, and boric acid	43.29%	1.34	28%
CG1-121	PADMAC and NaCl	36.96%	2.06	41%

The amount of free-radical initiator AIBN, crosslinking agent DVB, and the procedure for polymerizing network II were examined next. All aqueous phases contained PADMAC and NaCl. For the bulk polymerizations, the beads were swollen in the monomer solution, filtered and then placed in a vial sparged with nitrogen. The vial was then placed in an 80 °C oil bath. The results are displayed in Table 3.

The percent solids is an important characteristic because it reveals how hydrophobic the IPN is. A low percent solids is desireable so that the IPN will be hydrophilic and the functional groups will have the capability to interact more freely with solutions. Also, the more DVB present, the more hydrophobic an IPN will be. A large amount of DVB will create a bead that is very dense. In the absence of chain transfer, the amount of initiator determines the number of polymer chains that will be produced. The 5 wt% AIBN will create a large number of shorter chains, while the 1 wt% AIBN will yield a smaller number of chains that are longer.

The IPNs produced by bulk polymerization were very difficult to use. The beads adhered to each other and force was necessary to break them apart, resulting in non-uniform shapes. The percent solids of the bulk IPNs and the 18 mol % DVB IPNs were the highest, as was expected. The greater amount of DVB or AIBN did not significantly increase the percent yield. Thus, increasing the percent yield would be investigated by other variables. The IPN CG1-140 with the lowest percent solids of 49.15% was considered to have the ideal initiator level of 2 wt % AIBN and the ideal crosslinking level of 10 mol % DVB. These levels of initiator and crosslinking agent were kept constant for the remaining experiments.

Table 3. Comparisons of Initiator, Crosslinking Agent, and Procedure.

Resin	AIBN	DVB	Procedure	Solids (%)	VIm Capacity	Yield (%)
CG1-121	1 wt %	18 mol %	suspension	66.96%	2.06	41%
CG1-131	1 wt %	18 mol %	bulk	76.63%	1.90	37%
CG1-140	2 wt %	10 mol %	suspension	49.15%	1.59	33%
CG1-141	2 wt %	10 mol %	bulk	66.63%	2.85	59%
CG1-132	5 wt %	18 mol %	suspension	78.98%	1.06	27%
CG1-133	5 wt %	18 mol %	bulk	91.48%	1.61	41%

To investigate increasing the percent yield, the monomer solution was made at concentrations of 4.25 M and 6.20 M of functionalized monomer in toluene. The toluene swells the xerogel polystyrene beads to a greater extent than the monomer solution alone. Then, more of the monomer would be absorbed into the beads and the percent yield would increase; however, a dramatic increase in the percent yield did not occur as shown in Table 4. The IPNs produced by solution polymerization with the monomers in toluene were not more homogeneous and easier to use relative to the bulk IPNs. Since the 4.25 M monomer solution in toluene yielded poltmers in slightly greater percent yield with low percent solids, it was adapted as standard.

IPNs consisting of vinylimidazole and different co-monomers were examined to determine if combining vinylimidazole with a more reactive monomer would increase the percent yield. All of the IPNs contained 2 wt % AIBN, 10 mol % DVB, and the functionalized monomers were 4.25 M in toluene. The results are shown in Table 5. Methyl methacrylate was the most important co-monomer investigated because it was expected that the ester could be hydrolyzed to yield a carboxylic acid. Also, methyl methacrylate is considered to be very reactive. The co-monomers analyzed did not drastically affect the percent solids; however, the monomer solution with 1:1 vinyl imidazole:methyl methacrylate did have an 81% yield. The poly(vinylimidazole-co-methyl methacrylate) IPNs will be examined more in depth in the section entitled "Hydrolysis of Interpenetrating Polymer Networks".

Table 4. Investigation of Monomer Solutions in Toluene.

Resin	Conc. in Toluene	Procedure	Solids (%)	VIm Capacity	Yield (%)
CG1-142	no toluene	suspension	59.15%	1.60	33%
CG1-141	no toluene	bulk	66.63%	2.85	59%
CG1-134	4.25 M	suspension	58.92%	2.20	43%
CG1-135	4.25 M	solution	64.63%	1.04	21%
CG1-138	6.20 M	suspension	67.73%	1.92	34%
CG1-139	6.20 M	solution	56.77%	0.93	16%

Table 5. Examination of Vinyl Imidazole with Co-Monomers.

Resin	Co-Monomer	Ratio	Solids (%)	Capacity	Yield (%)
CG1-161	Styrene	1:1	74.06%	1.47	51%
CG1-164	Acrylamide	1:1	65.44%	1.33	39%
CG1-144	Methyl Methacrylate	1:1	58.40%	2.37	81%
CG1-198	Methyl Methacrylate	3:1	62.74%	2.11	47%
CG1-202	Methyl Methacrylate	5:1	59.09%	2.88	58%

Table 6 shows the results of the investigation of an aqueous phase developed by Dr. Andrezj Trochimczuk and tested by D. W. Crick. The new aqueous phase contained poly(vinyl alcohol) or PVA, and $CaCl_2$ in water. The percent yield was doubled and the percent solids was slightly lowered using the new aqueous phase. The vinyl imidazole did not leach out as was seen with the previous aqueous phase. This insolubility could be attributed to several factors. The PVA creates a more viscous solution than the PADMAC, and the $CaCl_2$ yields a solution with a higher ionic strength than the NaCl. Also, more of the $CaCl_2$ can be used than NaCl because it has a greater solubility in water.

The 5 mol % DVB was examined to determine if the percent solids could be lowered and to alleviate any future accessibility problems. However, more of the vinyl imidazole was incorporated with the 10 mol % DVB, and the percent solids was not greatly lowered. Also, the 10 mol % DVB helps to minimize phase separation of the two networks. If more entanglements are present by the crosslinking agent, less separation will occur between the two networks.

From these experiments, it was found that the vinyl imidazole IPN with the lowest percent solids and greatest percent yield was synthesized with 2 wt % AIBN, 10 mol % DVB, and at a concentration of 4.25 M of functionalized monomers in toluene using an aqueous phase consisting of PVA and $CaCl_2$ (IPN CG2-038, Table 6).

Table 6. Comparison of Aqueous Phases and Level of Crosslinking.

Resin	DVB	Aqueous Phase	Solids (%)	Capacity	Yield (%)
CG1-134	10 mol%	PADMAC and NaCl	61.92%	2.20	43%
CG2-038	10 mol%	PVA and $CaCl_2$	54.99%	4.38	83%
CG2-032	5 mol%	PVA and $CaCl_2$	52.37%	4.02	70%

Hydrolysis of Interpenetrating Polymer Networks

Methyl methacrylate (MMA) is hydrolyzed to obtain a carboxylic acid moiety. MMA polymerizes easily, and an 81% yield of VIm was achieved with MMA as the co-monomer. Several MMA IPNs (with xerogel polystyrene as network I) were synthesized, and the hydrolyses were attempted as shown in Table 7. None of the IPNs were hydrolyzed and all had high percent solids.

Hydrolysis of IPNs with network II consisting of different ratios of VIm and MMA were attempted. Also, 5, 10, and 20 mol % DVB crosslinking levels of the 1:1 VIm:MMA IPN underwent hydrolysis. All of the IPNs refluxed with 12 N HCl for 48 hours with the results shown in Table 8.

The 1:1 VIm:MMA IPNs with 5 and 10 mol% DVB (CG1-215 and CG1-148) showed a marked increase in the percent yield with values of 47% and 65%, respectively. The 20 mol % DVB IPN (CG1-213) has the highest percent solids, and its density may have hindered hydrolysis. Gozdz[67] found that the sensitivity of a methyl methacrylate monomeric unit to hydrolysis can be correlated with its environment in the polymer chain. The introduction of other monomers into the poly(methyl methacrylate) chain facilitates hydrolysis. The hydrolysis of CG1-148 may also be explained by the work by De Loecker[68] and Smets. They described the hydrolysis of poly(MMA) when optimum concentrations of methacrylic acid were present in the polymer chain and the intramolecular nature of the reaction mechanism involved. The carboxylic acid moiety of the methacrylic acid facilitated the hydrolysis of the ester portion of the methyl methacrylate.

Table 7. Attempted Hydrolyses of MMA IPNs.

Resin	Hydrolysis Procedure	Hyd. MMA Capacity (meq/g)	Solids (%)	Yield (%)
CG1-153[1]	12 N HCl/ 48 h	0.26	91.52%	4%
CG1-170[2]	12 N HCl/ 48 h	0.0	87.75%	0%
CG1-171[3]	12 N HCl/ 48 h	0.0	88.57%	0%
CG1-175[4]	12 N HCl/ 48 h	0.0	93.06%	0%
CG1-184[4]	12 N HCl/ 96 h	0.0	90.52%	0%
CG1-190[4]	1 N NaOH/ 48 h	0.0	86.96%	1%

[1]synthesized with 2 wt % AIBN, 4.25 M solution in toluene by suspension polymerization

[2]synthesized with 5 wt % AIBN, 4.25 M solution in toluene by suspension polymerization

[3]synthesized with 5 wt % AIBN, 4.25 M solution in toluene by bulk polymerization

[4]synthesized with 5 wt % AIBN, 4.25 M solution in toluene by suspension polymerization

Table 8. Attempted Hydrolyses of VIm-MMA IPNs.

Resin	VIm:MMA Ratio	DVB	Solids (%)	Hyd. MMA Capacity	Yield (%)
CG1-205	5:1	10 mol %	58.08%	0.14	14%
CG1-204	3:1	10 mol %	64.55%	0.0	0%
CG1-217	1:3	10 mol %	70.17%	1.01	20%
CG1-148	1:1	10 mol %	53.69%	2.10	65%
CG1-213	1:1	20 mol %	70.30%	0.32	13%
CG1-215	1:1	5 mol %	54.87%	1.69	47%

Methacrylic acid (MAA) was briefly investigated as a co-monomer with VIm. First, an IPN with xerogel polystyrene as network I and poly(methacrylic acid) as network II was synthesized. The resulting beads were in clumps and were heterogeneous as evidenced by beads with different shapes and colors. An IPN with VIm-MAA as network II was also heterogeneous, and the beads disintegrated during conditioning. Conditioning consists of washing the beads with water, 4 wt % NaOH, water, 4 wt % HCl, and water.

Ethyl acrylate (EA) was then examined as the co-monomer with VIm. The beads were synthesized with the same formulation as the VIm IPNs (10 mol% DVB, 2 wt% AIBN, and a 4.25 M solution in toluene). EA has the advantages of being a very reactive monomer, and both the ester and acid derivatives (obtained after hydrolysis) could be studied with VIm. The hydrolysis procedures that were investigated with the IPNs having poly(ethyl acrylate) as network II are shown in Table 9. The greatest percent yields were obtained with the KOH in dioxane solutions. The dioxane swelled the beads which facilated the hydrolysis. It also appeared important that the solution was rapidly refluxing. The agitation resulted in slightly higher percent yield, but the percent solids remained the same.

In addition to the wet chemistry techniques, the hydrolysis of the bifunctional VIm-EA IPNs and the EA IPNs was confirmed by solid-state ^{13}C NMR spectroscopy by Crick and Alexandratos[30]. Ethyl acrylate was chosen as a co-monomer with vinyl imidazole for the final set of IPNs whose microenvironment was examined with small molecules and metal ions.

Table 9. Hydrolysis Procedures for Ethyl Acrylate IPNs.

Resin	Hydrolysis Procedure	Solids (%)	Hyd. EA Capacity (meq/g)	Yield (%)
CG1-221	12 N HCl/48 h	79.28%	1.51	21%
CG2-030	2 N KOH in Dioxane/24 h 12 N HCl/24 h	62.54%	5.18	70%
CG2-036	2 N KOH in Dioxane/ 40 h	48.43%	5.10	69%
CG2-172	2 N KOH in Dioxane/ 56 h	58.45%	5.18	79%
CGC3-072	2 N KOH in Dioxane/ 56 h rapidly refluxing	58.85%	5.49	87%

Characterization of Interpenetrating Polymer Networks

To determine the capacity of the VIm IPN, both the protonated and the unprotonated multiply bonded ring nitrogen sites must be measured after the beads have been conditioned. In the conditioning process, one liter each of H_2O, 4 wt % NaOH, H_2O, and 4 wt % HCl is eluted. At this time all of the sites are protonated. Then, H_2O is eluted until pH paper displays a pH of approximatly 5 to 6. Imidazole has a pK_a of 7.00[59], and the water will partially deprotonate the multiply bonded ring nitrogen sites. The acid capacity and base capacity measure the acid and base sites, respectively. The total anion-exchange capacity (TAEC) measures the chloride that is the counterion to the protonated imidazole; therefore, it is equal to the acid capacity for the VIm IPN.

The capacity of the bifunctional VIm-hydrolyzed EA IPN is found in a similar manner. As with the monofunctional IPN, the beads are conditioned with the same procedure, and an acid capacity, base capacity, and TAEC are completed. The base capacity gives the milliequivalents of unprotonated imidazole sites, the TAEC provides the milliequivalents of the protonated imidazole sites, and the acid capacity less the TAEC yields the milliequivalents of hydrolyzed ethyl acrylate.

The IPNs are also characterized with infrared spectroscopy. Figure 6 displays the IR spectrum of a VIm IPN, and Figure 7 contains 3 overlaid spectra including an EA IPN, 1:1 VIm:EA IPN, and VIm IPN. In Figure 7, the C=O stretch at 1720 cm^{-1} is broad and strong for the EA IPN and less broad but still strong for the VIm-EA IPN.

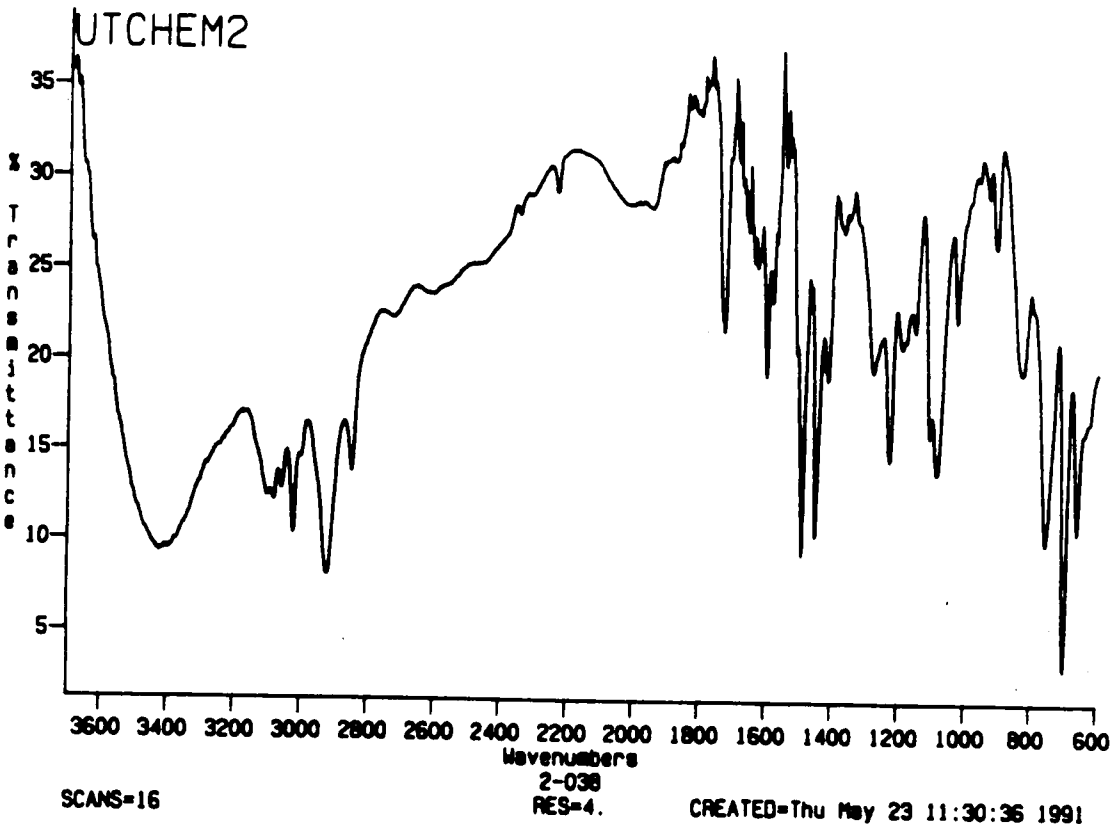


Figure 6. Infrared Spectrum of VIm IPN.

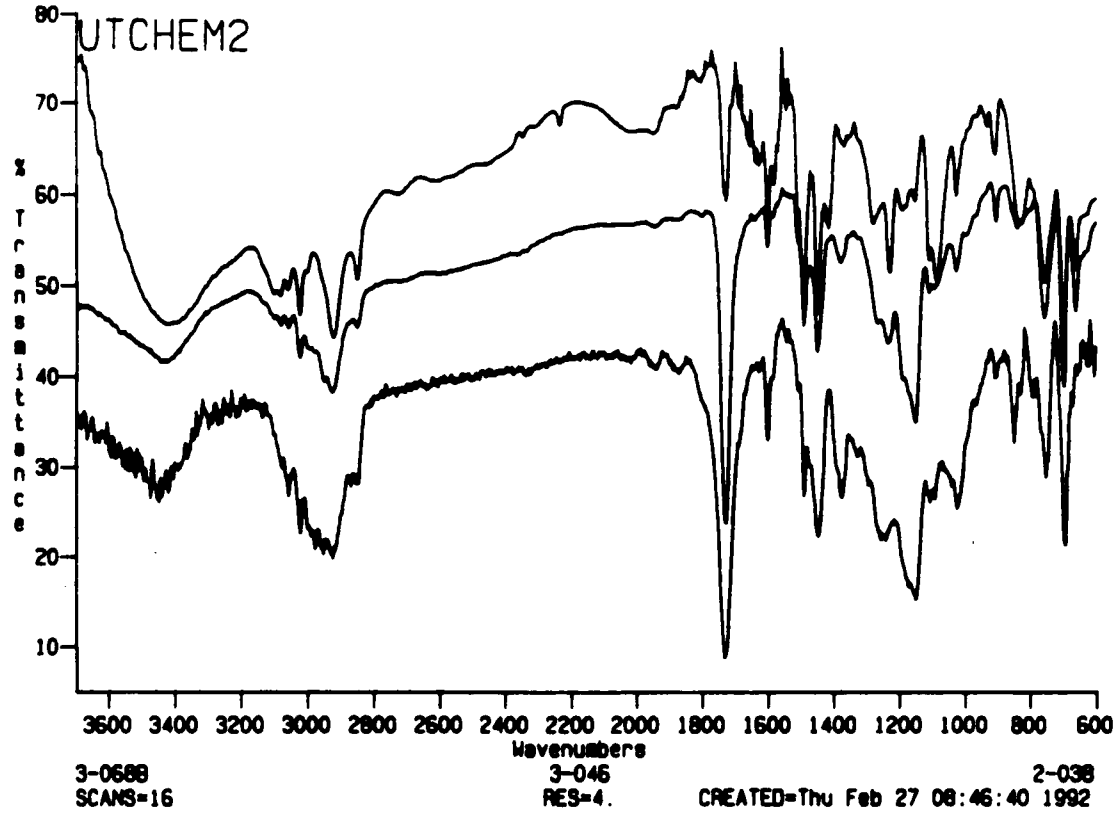


Figure 7. Infrared Spectra of (bottom to top) EA IPN (3-068B), VIm-EA IPN (3-046), and VIm IPN (2-038).

Figure 8 contains IR spectra of hydrolyzed EA IPN, hydrolyzed 1:1 VIm:EA IPN, and VIm IPN. Again, a noticeable change can be seen at approximatly 1720 cm^{-1}. In Figure 9, the IR spectrum of the VIm-EA IPN is compared to its hydrolyzed product, which shows a broad peak at 2500 cm^{-1} indicative of hydrogen bonding[69] between the acid and acid/imidazole ligands. The C=O peak at 1720 cm^{-1} broadens after the hydrolysis as was seen in the previous spectra.

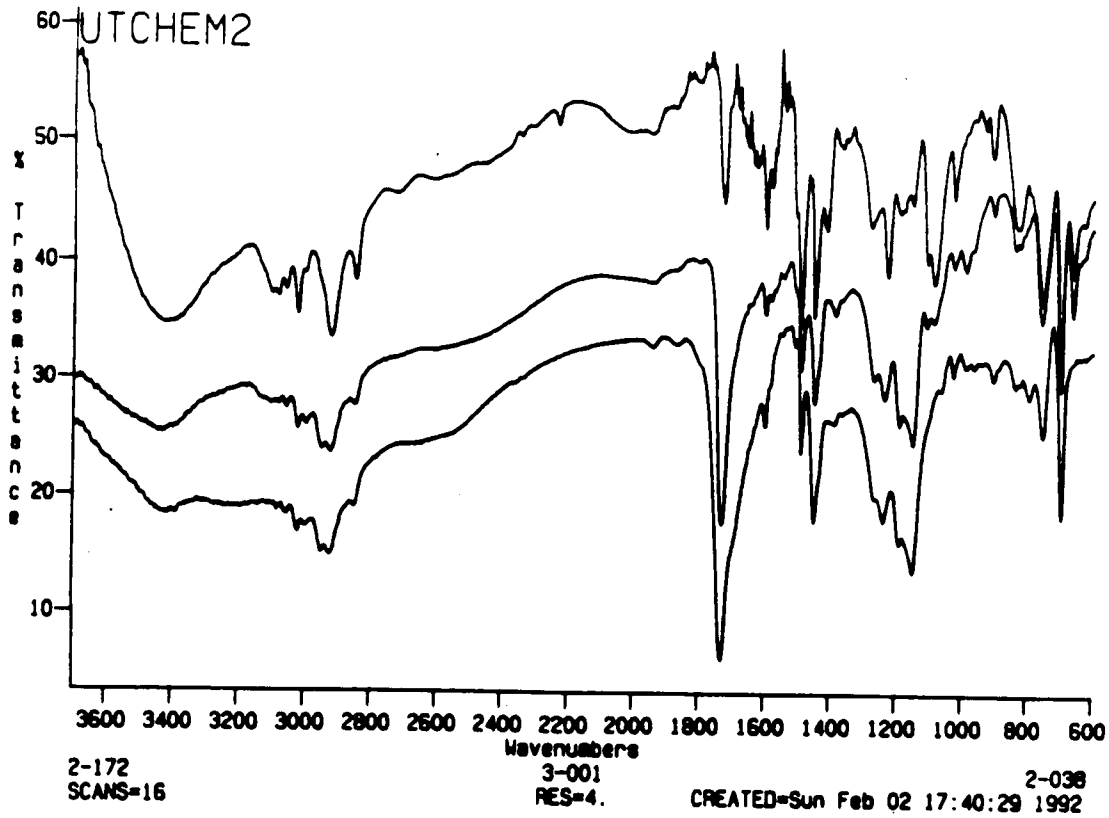


Figure 8. Infrared Spectra of (bottom to top) Hydrolyzed EA IPN (2-172), Hydrolyzed VIm-EA IPN (3-001), and VIm IPN (2-038).

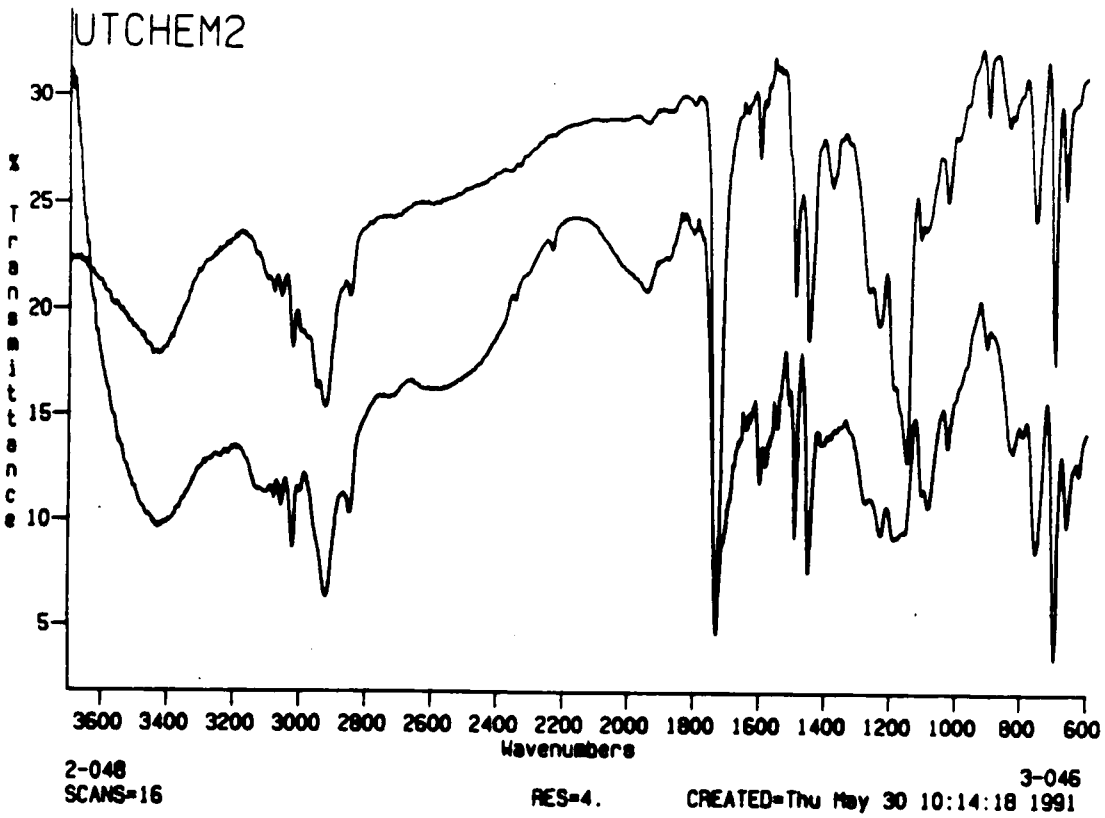


Figure 9. Infrared Spectra of (bottom to top) Hydrolyzed VIm-EA IPN (2-048) and VIm-EA IPN (3-046).

CHAPTER III

MOLECULAR RECOGNITION

Introduction

The design and synthesis of polymer-supported reagents for molecular recognition studies is important to fundamental chemistry, given its focus on defining ligand-molecule interactions, and to applied chemistry, given its utility for biomolecular separations. The majority of biological macromolecules are capable of recognizing, or being recognized by, other molecules present in biological systems. Affinity chromatography relies on the highly specific molecular interactions involved in biological recognition. After the development of suitable polymeric supports, affinity chromatography became a routine tool for protein purification[3]. Organic and inorganic polymer supports have been used for the anchoring of chiral stationary phases that are employed in the chromatographic separation of enantiomers[3].

Molecular complexations with polymer-supported reagents depend not only on the nature of the ligand, but also on the microenvironment surrounding each ligand[70]. Crosslinked macromolecules, functionalized by template synthesis method,

use molecular recognition as the principal diagnostic to evaluate maintenance of the stereochemical integrity of functional groups[71]. In a similar manner, molecular recogniton studies with phenylphosphinic acid were completed as probes of the microenvironment of a series of VIm-EA IPNs. The series consisted of IPNs with 25%, 53%, 76%, and 100% VIm with the remaining polymer comprised of ethyl acrylate. Langmuir isotherms and binding constants were calculated for each ligand-substrate interaction. The binding constants or K_{11}'s are derived in the Appendix.

In a companion study, polymer-supported dimethylamine ligands were studies due to its well-defined ligand structure. The microenvironment of the dimethylamine (DMA) ligands was varied by the crosslinking level and by the percent functionalization. The partially functionalized resins were also investigated with polar and nonpolar solvents, methanol and 1,4-dioxane, in the molecular recognition studies. The target molecules for the DMA resins were substituted benzoic acids, and the binding constants obtained from these studies were used in Hammett-type correlations.

The Microenvironmental Effect of Vinyl Imidazole-Based Interpenetrating Polymer Networks

To investigate the microenvironmental effect, a series of IPNs were utilized that possessed different ratios of VIm and EA which varied the polarity in the resin. The mole ratios of VIm and EA in the monomer solution that swelled the xerogel polystyrene were varied to achieve the different amounts of functional groups on

network II. The VIm capacity was determined with an acid capacity, base capacity, and TAEC. The EA capacity was determined by back-calculating from the acid capacity after ester hydrolysis.

Swelling ratios were obtained in both a polar and nonpolar solvent in order to quantitatively describe the polarity of the resins. First, the beads were dried in a vacuum oven for 17 hours and then placed in a 10 mL graduated cylinder with the appropriate solvent. An initial volume of the beads was noted, and any air bubbles present were removed by gentle stirring. After swelling 24 hours, a final volume of the beads was recorded. All swelling ratios were obtained at room temperature. The swelling ratios were found by dividing the final volume by the initial volume and are shown in Table 10.

Methanol, which has a dielectric constant of 32.6 (at 25 °C), was the polar solvent utilized, and 1,4-dioxane, which has a dielectric constant of 2.21 (at 25 °C), was the nonpolar solvent. The 100% VIm IPN had the largest swelling ratio in methanol and the smallest in dioxane; therefore, the microenvironment with no ethyl acrylate groups possessed the greatest polarity. Likewise, the 100% EA IPN swelled the most in dioxane and the least in methanol and thus exhibited the smallest amount of polarity in the beads. The fact that VIm is more polar than EA can be explained by the ability of the protonated imidazole to hydrogen bond and the ring nitrogen's free lone pair orbital which is located in the plane of the ring.

Polymer-solvent systems can also be described quantitatively by the Flory-Huggins parameter, χ. Positive values of χ indicate that replacement of a solvent

molecule by a polymer molecule occurs with a positive enthalpy change (i.e., is an endothermic process). Negative values of χ would indicate exothermic dissolution and are observed very rarely. Negative χ values are more likely in systems in which the polymer and solvent are polar (thereby increasing the attractive interactions on mixing). Thus, the 100% VIm IPN in methanol would have a smaller value of χ than the 100% VIm IPN in 1,4-dioxane.

Table 10. Swelling Ratios of VIm-EA IPNs in Methanol and 1,4-Dioxane.

Resin	% VIm	Swelling Ratio in Methanol	Swelling Ratio in 1,4-Dioxane
CG2-178	100%	1.88	1.00
CG2-212B	76%	1.50	1.00
CG2-280B	53%	1.67	1.40
CG2-232	27%	1.67	1.75
DC3-267[1]	0%	1.00	2.58

[1]100% EA IPN.

The procedure for the molecular recognition studies is described in detail in Chapter 5. Briefly, one milliequivalent (meq) of the desired IPN was contacted with 10 mL of phenylphosphinic acid (PPA) in methanol. The concentration of the PPA was varied to give a wide range of R_i values (R_i = meq of PPA/meq of ligands within the IPN). After contacting 17 hours, the PPA was titrated to determine the amount of the acid remaining in solution and hence, the amount complexed by the resin. The values of r (meq of PPA bound/grams of dry resin) and c (meq of PPA free/ml of solution) were determined and graphed in order to obtain the saturation capacity (S_t) of the resin. The complexation data, r and c, are then fitted to a modified Langmuir isotherm equation, and the binding constant K_{11} was then calculated from the *y*-reciprocal form of the Langmuir equation. The K_{11} represents the strength of the interaction or binding between the two groups. A more detailed explanation and derivation of the K_{11}'s can be found in the Appendix.

The r vs. c curves for the different VIm-EA IPNs with PPA are shown in Figure 10. The 100% VIm IPN has the greatest S_t while the 27% VIm has the lowest S_t. From the *y*-reciprocal plot (c/r vs. c) shown in Figure 11, the K_{11} was obtained by using equation 1.

$$K_{11} = \frac{slope}{intercept} \tag{1}$$

The binding constants, saturation capacities, and measured VIm capacity of the VIm-EA IPN series are displayed in Table 11.

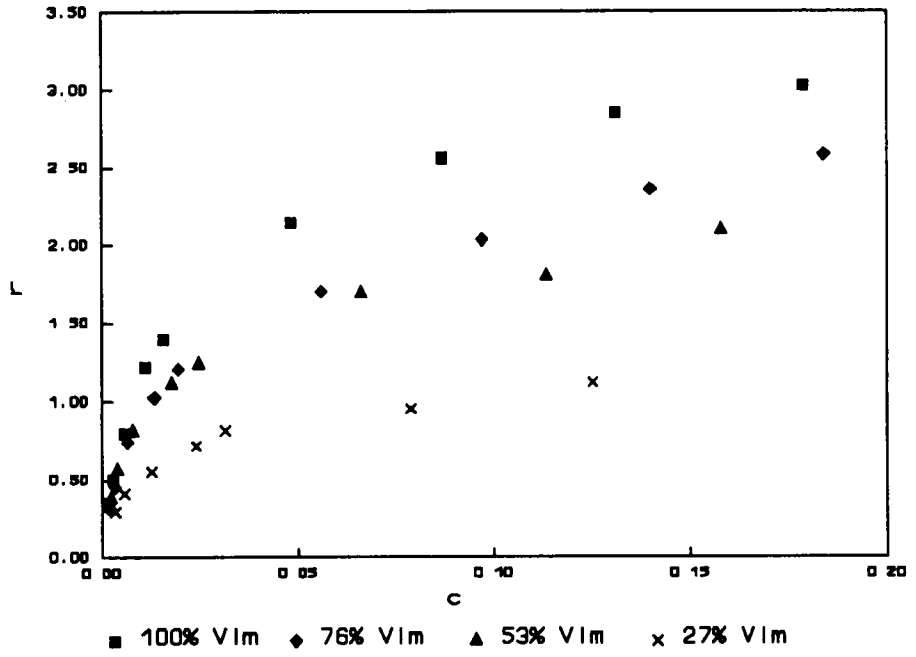


Figure 10. Adsorption Isotherms for VIm-EA IPNs with PPA.

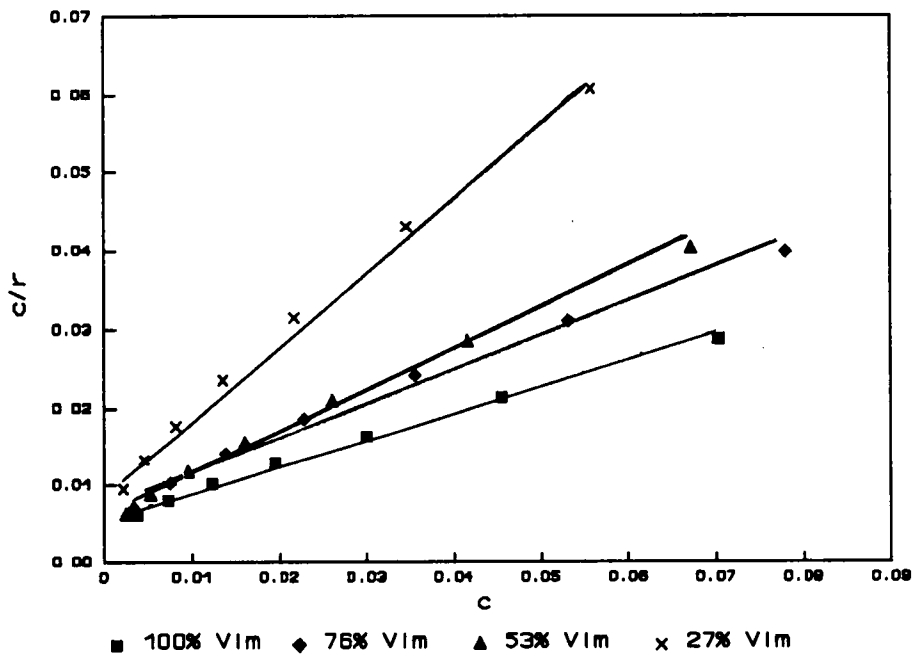


Figure 11. *y*-Reciprocal plots for VIm-EA IPNs with PPA.

Table 11. Binding Constants of VIm-EA IPNs and PPA.

Resin	% VIm	VIm Capacity	S_t	K_{11} (N^{-1})
CG2-178	100%	4.60	3.05	58.82
CG2-212B	76%	3.02	2.45	57.80
CG2-280B	53%	2.65	2.10	84.85
CG2-232	27%	1.22	1.15	98.32

The 27% VIm IPN had the greatest K_{11} (98.32 N^{-1}) which represents the strongest complexing of PPA in the series. The weakest interactions were with the 76% VIm and the 100% VIm IPNs which had K_{11}'s of 57.80 N^{-1} and 58.82 N^{-1}, respectively. The 53% VIm resin resulted in an intermediate binding of 84.85 N^{-1}. The S_t of the 100% VIm IPN is 66% of its true capacity, and the 76% and 53% VIm beads are very similar in this respect with S_t's 81% and 79% , respectively, of their measured capacity. Almost every imidazole group in the 27% VIm IPN was binding PPA which is indicated by the fact that the S_t is 94% of the true VIm capacity.

Thus, the 27% VIm-EA IPN bound the PPA the strongest, and the greatest percentage of its imidazole groups were involved. This may be explained by the polarities of the IPNs and the choice of methanol as the solvent. The more polar imidazole groups were solvated by the methanol as was the PPA. As the polarity of the resin decreased (due to a decrease in the number of imidazole groups), the methanol did not have the same stabilizing affect. However, the resin was "solvated" by the acid-base interaction between the imidazole and PPA and thus, the stronger binding. Therefore, the IPN with the fewest number of imidazole groups would have the greatest K_{11}, which was observed.

Additional molecular recognition studies were conducted with the VIm-EA IPN series. The resins were contacted with benzenesulfonic acid, but the interaction was too strong to be measured by our methods. The r vs. c curve possessed a very steep rise which resulted in a negative intercept on the *y*-reciprocal plot.

The Microenvironmental Effect of Dimethylamine Resins

The Hammett Equation in Molecular-Recognition Studies

To determine the extent to which the ligand-substrate interaction depends upon the microenvironment surrounding polymer-supported ligands, molecular binding studies within a Hammett-type correlation were also conducted. The Hammett equation gives information that is a measure of the interaction's sensitivity to electron density changes. We have applied this idea to a comparison of the sensitivities across different matrices in order to provide a measure of how the polymeric microenvironment influences that sensitivity.

The Hammett equation was used for several reasons, the most important being that the substrate acidity can be varied while minimally changing the overall molecular structure. Also, the equation allows quantitative treatment of the data. In this study, polymer-supported dimethylamine ligands were contacted with substituted benzoic acids. The strength of the functional group (carboxylic acid) was varied by changing the electron density at the reactive site by using electron-withdrawing and electron donating substituents.

The Hammett equation, equation 2, is a linear free-energy relationship, and provided that all other variables are kept constant while one is systematically

$$\log K^x/K^H = \sigma \rho \qquad (2)$$

varied, will yield a direct comparison of the reactivity of similar compounds whose only difference is the electron density at the functional group. In this equation, σ is the substituent constant, and ρ is the reaction constant. K^X and K^H are the equilibrium or binding constants for the substituted and the unsubstituted reactions, respectively. Therefore, it can be seen that if the interaction using the substituted species is faster or stronger than the unsubstituted species, the absolute value for ρ will increase. Since the equation was originally devised to explain the ionization of benzoic acids in water (which is assisted by electron-withdrawing groups, thereby increasing the ratio K^X/K^H), positive σ values indicate electron-withdrawing groups, while negative σ values denote electron-donating groups. Thus, positive ρ values signify that the reaction is aided by electron-withdrawing groups, and negative ρ values indicate that the reaction is helped by electron-donating groups.

The Effect of Partial Functionalization

The effect of partial functionalization was investigated with a 100% substituted dimethylamine (DMA) resin and a 40% substituted DMA resin (the remaining portion consisting of polystyrene). The percent substitution governed the polymer's overall polarity, and both resins were crosslinked with 2wt% DVB.The substrates were a series of benzoic acids with substituents (*p*-CH_3, *m*-CH_3, H, *m*-CH_3O, *p*-Cl, and *m*-Cl) used to adjust the hydrogen-bonding ability of the functional group. The tendency of each substituent to act as an electron donor or withdrawer is quantified by its Hammett sigma constant[72] (-0.14, -0.06, 0, 0.10, 0.24, and 0.37 for

the substituents in the order listed above). The 100% DMA resin (with a capacity of 5.15 meq/g) was contacted with all of the substituted benzoic acids mentioned earlier; however, the 40% substituted DMA resin (capacity of 2.19 meq/g) was contacted with only the *p*-CH_3, H, *p*-Cl, and *m*-Cl.

The procedure for the DMA molecular recognition studies was identical to that of the VIm IPN contacted with PPA. All studies were conducted in methanol. From the % complexed by the ligand, the complexation data r and c were obtained. Figure 12 shows the binding (r vs. c) curve for the 40% DMA resin interaction with the *p*-CH_3, H, and *m*-Cl substituted benzoic acids, and the corresponding *y*-reciprocal plots are in Figure 13. The adsorption isotherm for the 100% DMA resin with the same substrates is displayed in Figure 14 with the corrresponding *y*-reciprocal plots shown in Figure 15. The binding constants obtained from the *y*-reciprocal plots are in Table 12.

The binding constants from the interaction of substituted ArCOOH and fully functionalized DMA polymer are found to increase with increasing substrate ability to hydrogen bond with the amine lone pair. The K_{11}'s range from a low of 32.13 N^{-1} (*p*-CH_3) to a high of 126.19 N^{-1} (*m*-Cl). As expected, the most electron-withdrawing substituent, which appropriately has the greatest positive Hammett sigma constant, had the largest K_{11} and thus, the strongest interaction. The 40% substituted DMA resin also had increasing binding constants with increasing Hammett constants. However, the increase was milder relative to the fully functionalized polymer. The lowest K_{11}

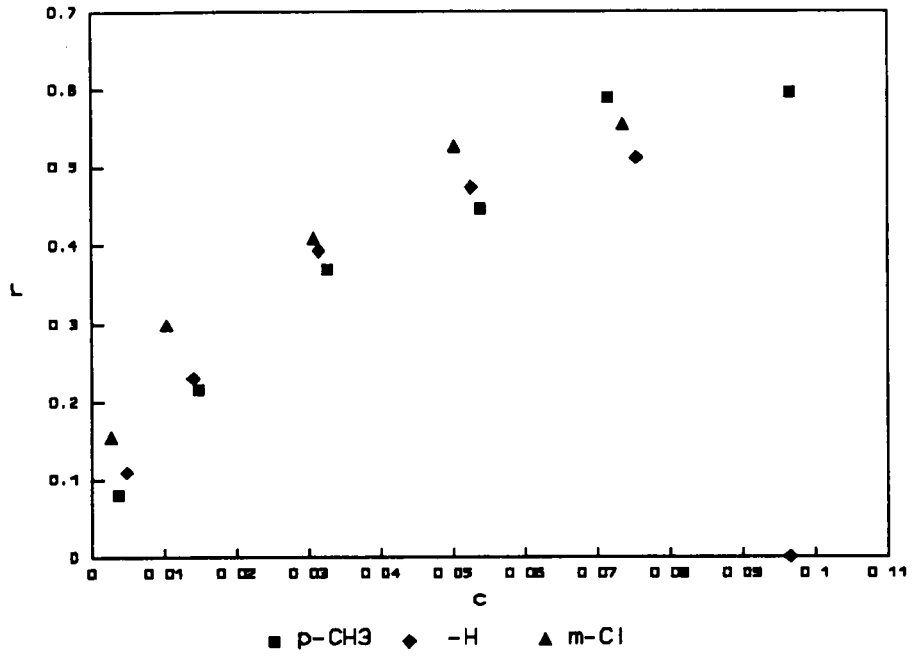


Figure 12. Binding Curve for 40% DMA with Substituted ArCOOH.

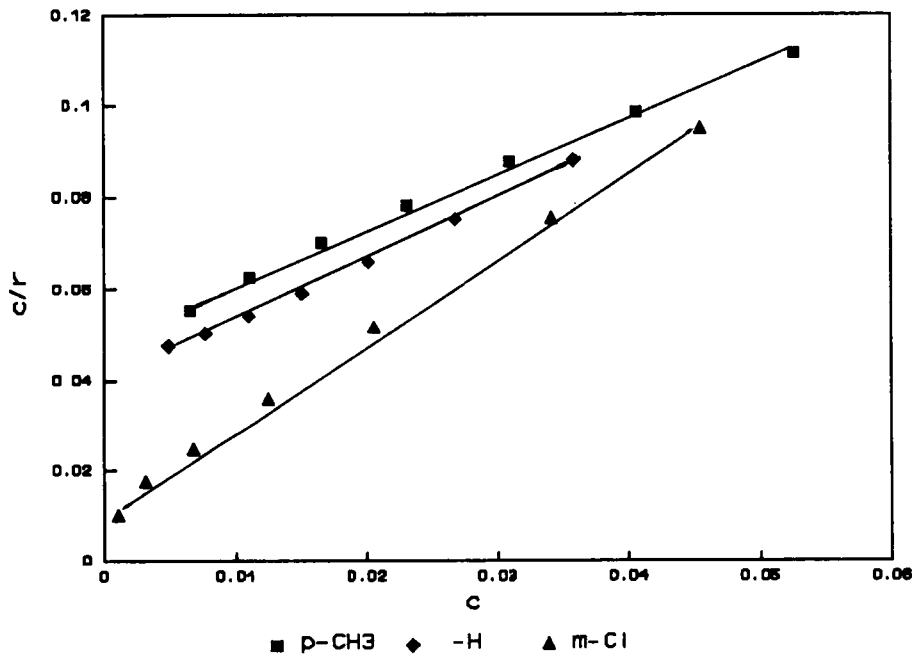


Figure 13. *y*-Reciprocal Plot for 40% DMA with Substituted ArCOOH.

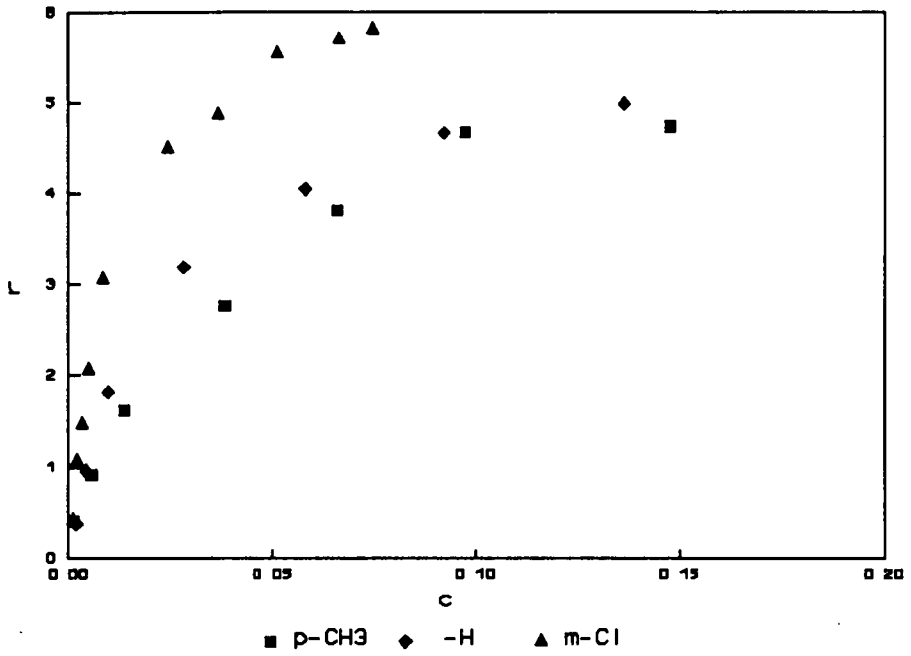


Figure 14. Binding Curve for 100% DMA with Substituted ArCOOH.

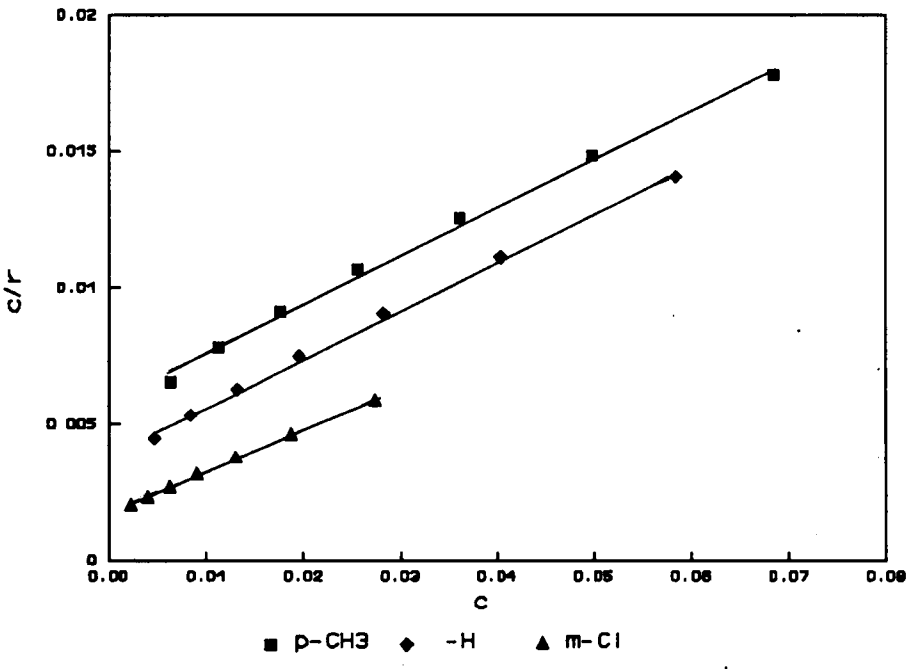


Figure 15. *y*-Reciprocal Plot for 100% DMA with Substituted ArCOOH.

Table 12. Binding Constants of 40% and 100% DMA Resins with Substituted ArCOOH.

Substituted ArCOOH	Hammett Constant	40% DMA K_{11} (N^{-1})	100% DMA K_{11} (N^{-1})
p-CH_3	-0.14	32.20	32.13
m-CH_3	-0.06	-	40.17
-H	0.0	38.01	51.07
m-OCH_3	0.10	-	61.94
p-Cl	0.24	68.55	92.56
m-Cl	0.37	97.85	126.19

was 32.20 N^{-1}, and again, the stongest interaction occurred with the *m*-Cl substituent resulting in a binding constant of 97.85.

Correlating the data within a Hammett-type relationship through the relative ratios of the binding constants (substituted acids, K^X, to benzoic acid, K^H) yields equation 3, where the slope now quantifies the interaction's sensitivity to electron density changes at the active site of the 100% DMA resin. Equation 3 is shown

$$\log(K^X/K^H) = 1.159 \text{ (sigma)} - 0.027 \qquad (3)$$

graphically in Figure 16. The Hammett plot for the 40% DMA resin in Figure 17 yields equation 4.

$$\log(K^X/K^H) = 0.980 \text{ (sigma)} + 0.038 \qquad (4)$$

Comparing the slopes of the 100% and 40% DMA resins resulted in the conclusion that decreasing the polarity of the microenvironment at a constant crosslink level leads to a 15% decrease in reaction sensitivity. Decreasing the degree of substitution decreases the polymer's polarity as measured by its ability to sorb low polarity solvents such as dioxane. Comparing 2% DVB-crosslinked 100% DMA substituted with 40% DMA substituted and unsubstituted polystyrene shows swelling ratios in dioxane of 1.19, 1.76, and 3.10, respectively; the increased sorption of a non-

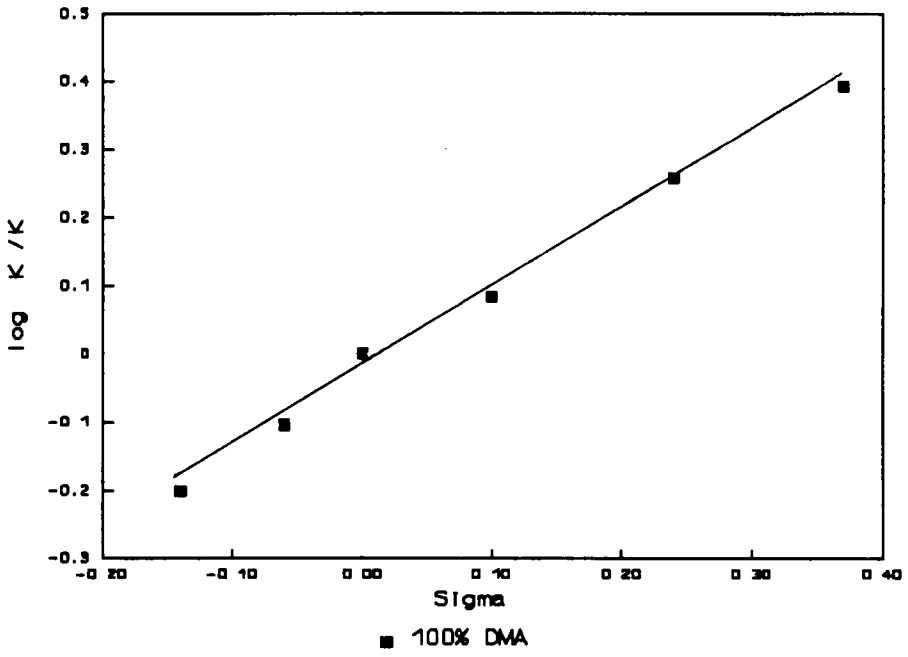


Figure 16. Hammett Plot of 100% DMA.

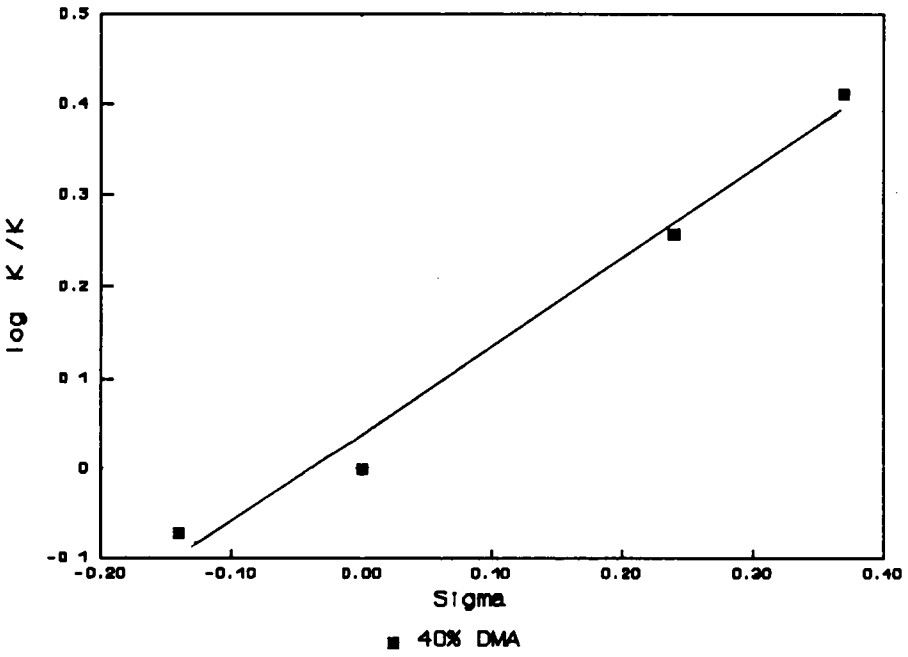


Figure 17. Hammett Plot of 40% DMA.

polar solvent with decreasing degree of substitution points to a decrease in the polymer's overall polarity.

The Effect of Solvent on Partially Functionalized Resins

Molecular recognition studies with 100% DMA substituted and 40% DMA substituted resins were also conducted in 1,4-dioxane, a low polarity solvent. The substituents on the benzoic acids examined were *p*-OCH_3, H, and *m*-Cl benzoic acid. The procedure followed the previuosly mentioned molecular recognition studies.

The adsorption isotherms for the 40% and 100% DMA resins are shown in Figure 18 and Figure 19, respectively. All of the r vs. c curves have a slow-rising, gentle slope. With the 40% DMA, a plateau or saturation capacity is apparently reached with the *p*-OCH_3 benzoic acid, but the unsubstituted acid and *m*-Cl continue to rise. This is also seen with the 100% DMA; the r values for higher R_i's (R_i = meq of acid/meq of resin) were much higher than the capacity of the polymer, 5.15 meq/g. Binding constants could not be measured due to the presence of this aspecific adsorption.

The aspecific adsorption can be attributed to the behavior of the solvent dioxane. Dioxane is only slightly polar while the amine ligand and benzoic acids are more polar. Therefore, dioxane does not stabilize the ligands or substrates individually or when they are in an even more polar complex; in fact, the complexation may be hindered by the dioxane. As the R_i increases, the concentration of the benzoic acid

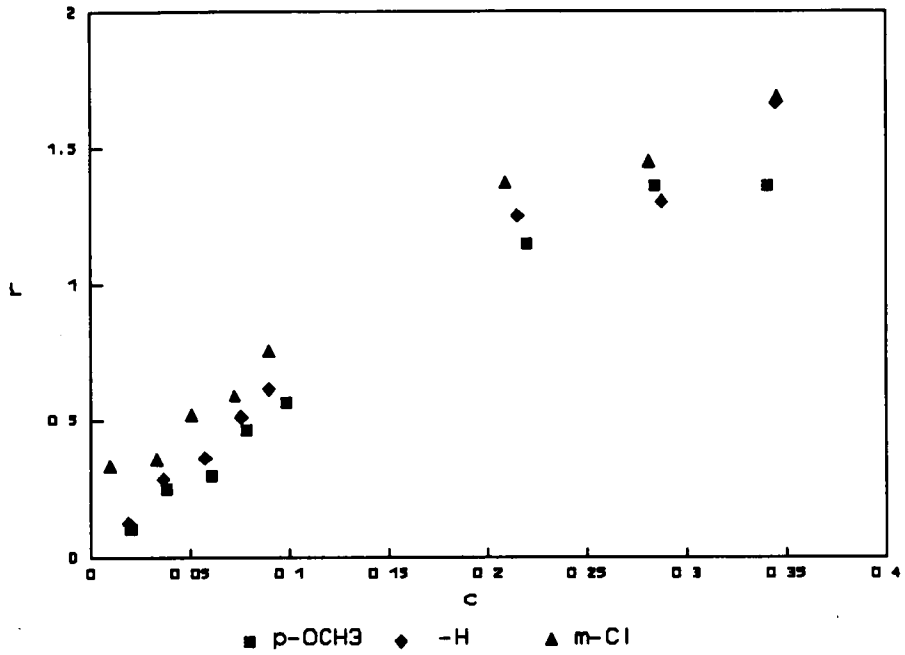


Figure 18. Adsorption Isotherm of 40% DMA with Benzoic Acids in 1,4-Dioxane.

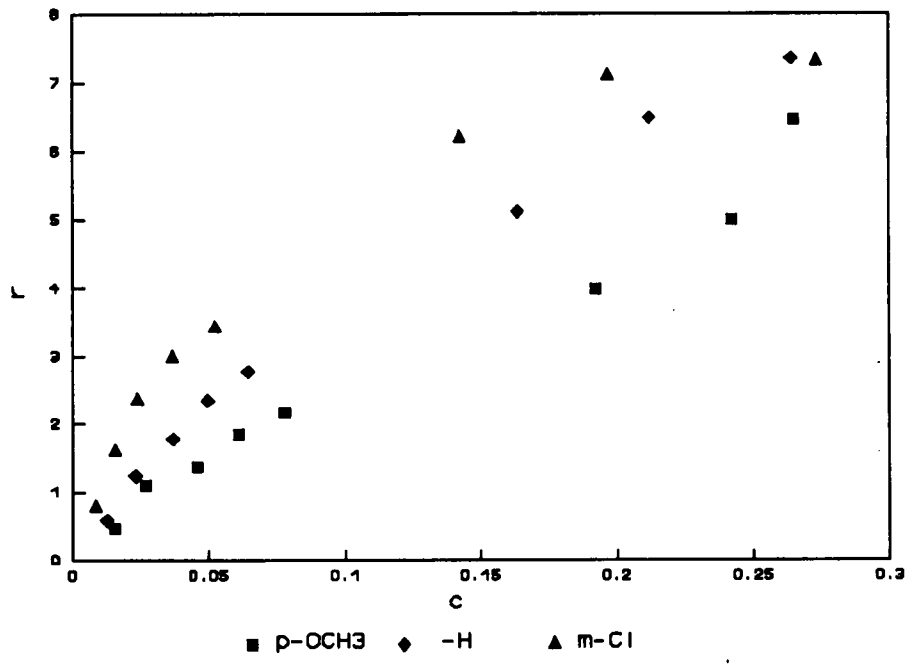


Figure 19. Adsorption Isotherm of 100% DMA with Benzoic Acids in 1,4-Dioxane.

increases, and the acid molecules aggregate around the amine ligands. This aggregation of several acid molecules to one amine ligand creates a dispersal of charge that can stabilize itself. With the 100% DMA resin, the amine ligands are very close to each other, and a dynamic equilibrium can occur with the acid molecules binding to one amine ligand and then another. However, with the 40% DMA resin the ligands are farther apart, and a dynamic equilibrium probably does not occur to the extent of the 100% substituted DMA. Thus, 1:1 binding was not taking place at the higher R_i's (higher portion of r vs. c curve). The Langmuir adsorption isotherm only applies to 1:1 complexation which explains why a clear plateau was not realized and binding constants could not be obtained.

The Effect of Crosslink Level

Molecular recognition studies were conducted with 2, 5, 10, 15, and 25% DVB dimethylamine polymers to investigate the effect of the crosslink level. All of the resins were 100% substituted with capacities of 5.15, 5.03, 4.46, 3.87, and 2.84 meq/g, respectively. The crosslink level did not affect the amination procedure. The % DVB does affect the network rigidity which was indicated by the swelling ratios of the series of polymers in toluene (2.8, 2.3, 1.5, 1.3, and 1.2, respectively).

The resins were contacted with 0.10 N, 0.05 N, and 0.01 N (R_i = 1.0, 0.5, and 0.1, respectively) methanolic solutions of *p*-anisic acid, *p*-toluic acid, *m*-toluic acid, benzoic acid, *m*-anisic acid, *p*-chlorobenzoic acid, and *m*-chlorobenzoic acid. The amount of each acid complexed by 1 meq of amine ligand at equilibrium was

correlated with the ligand's Hammett constant (-0.28, -0.14, -0.06, 0, 0.10, 0.24, and 0.37 for the acids above). The procedure followed that of the previously discussed molecular-recognition studies.

Network rigidity affects the percent complexed at an R_i of 1.0, with increasing rigidity decreasing the sorption capacity in the order 2% > 5% > 10% > 15% > 25% DVB as shown in Figure 20. The lower percent complexed with increasing crosslink level can be due to the network's inability to accomodate higher levels of substrate. The dimethylamine ligand's sensitivity to electron density at the substrate's functional group is unaffected by network rigidity, at least to 15% DVB, as seen by the similar correlations as the DVB level is varied. The most highly crosslinked resin, at 25% DVB, is almost completely unable to distinguish among the different benzoic acids. It is thus possible that a level of network rigidity can be attained which will accomadate a minimum amount of substrate due to steric crowding within the network, regardless of the ligand-substrate affinity.

At an R_i of 0.1, with a ten-fold excess of ligands to substrates, the polymer network plays a critical role in setting the molecular recognition pattern: as the network crosslinking increases over 5% DVB, the specificity of the ligand-substrate interaction increases, given the increased steepness in the percent complexed vs. sigma curve shown in Figure 22. The resin performance from the R_i 0.5 solutions is intermediate to that of the other two conditions as shown in Figure 21. The 2% DVB and 5% DVB results are identical to those at the lowest R_i but otherwise the influence of network rigidity is comparable to the higher R_i.

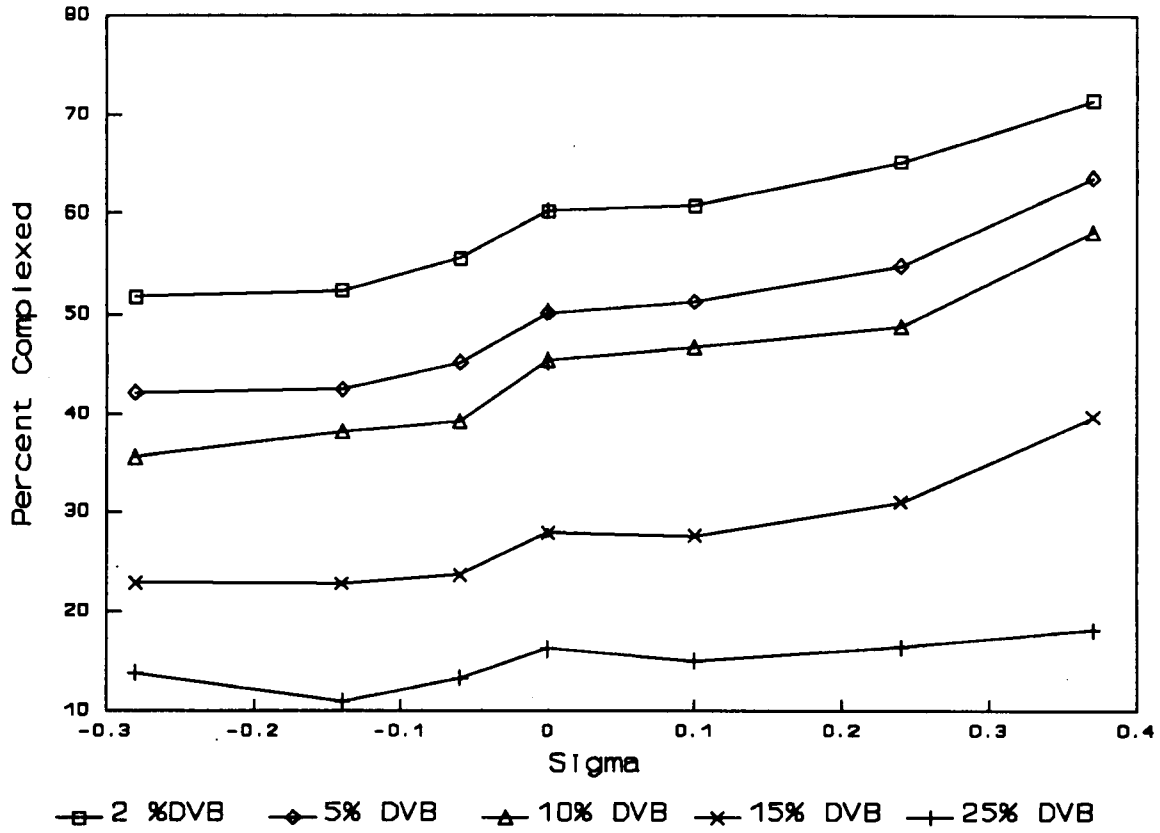


Figure 20. Percent Complexed by DMA Resins of Substituted ArCOOH at R_i = 1.0.

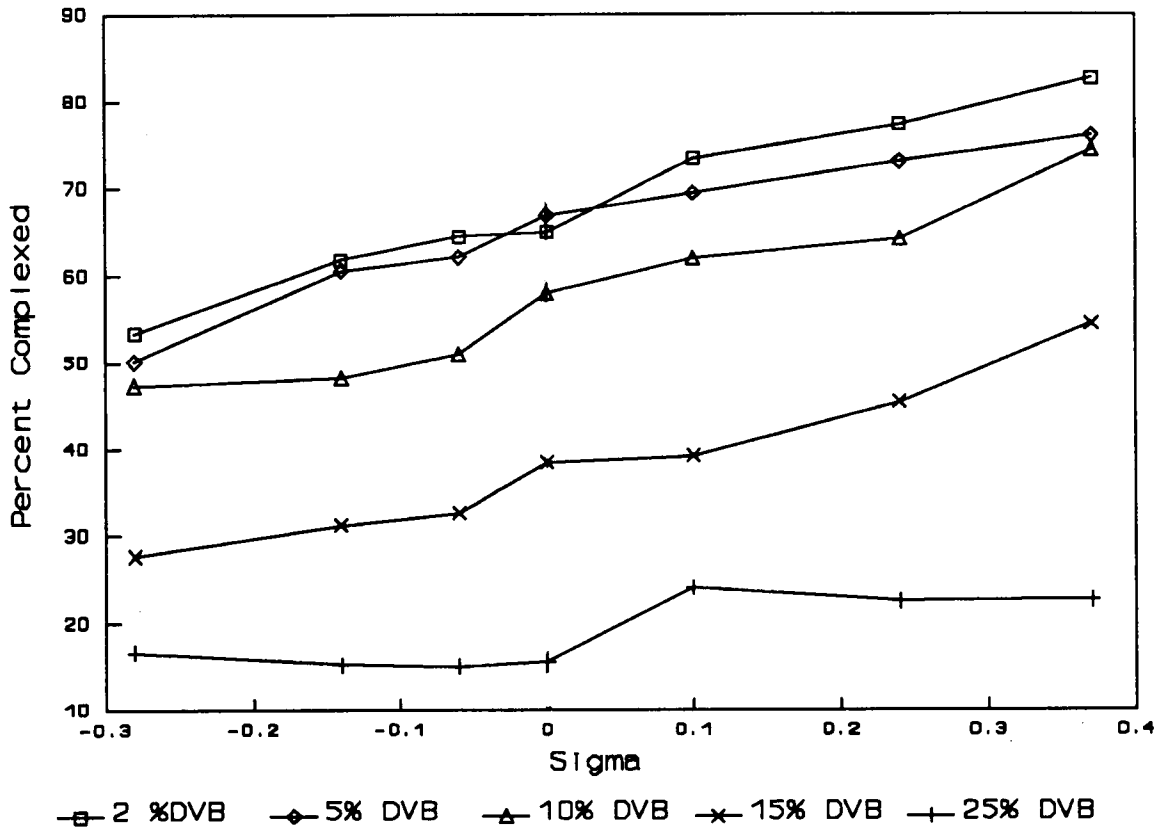


Figure 21. Percent Complexed by DMA Resins of Substituted ArCOOH at R_i = 0.5.

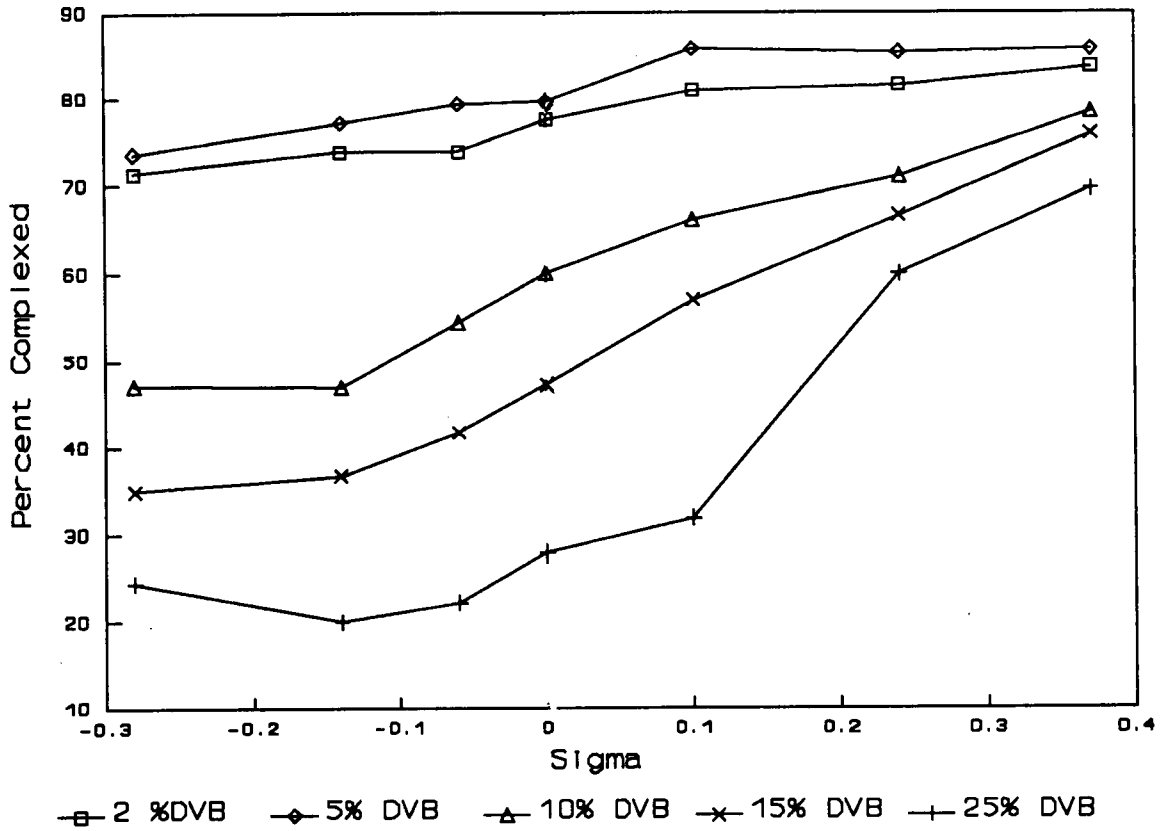


Figure 22. Percent Complexed by DMA Resins of Substituted ArCOOH at R_i = 0.1.

Conclusions

Molecular-recognition studies are an important tool for investigating a functionalized polymer or IPN. Binding constants from these experiments give insight to the microenvironment around the ligand. While the ligand-substrate interaction is an important factor in determining the binding constant, the polymeric microenvironment plays an equally critical role in the overall value as was demonstrated with the VIm IPNs and PPA, which showed that the least polar IPN had the strongest interaction with the PPA. Utilizing the combination of binding constants and the Hammett equation yielded even more information about the DMA resins. In that study, the ligand-substrate interaction's sensitivity to electron density changes at the active site were quantified, and resins with different polarities were compared. The less polar network, the 40% substituted DMA, showed a decrease in reaction sensitivity to changes in the electron density at the binding site. Thus, molecular recogniton experiments have been proven to be valuable in understanding the microenvironment in supported species.

CHAPTER IV

IONIC RECOGNITION

Introduction

Polymer-supported reagents play an important role in the coordination chemistry of metal ions as applied to environmental separations and chemical sensors. The chemistry of complexing resins began in the late 1940's when a polystyrene supported dipicrylamine group was developed and found to be specific for potassium ion[20]. This has been followed by an increasing utility and application of complexing resins in transition, alkali and alkaline earth metal ion separations, preconcentation and recovery of trace metal ions, catalysis, hydrometallurgy, and in analytical chemistry[20].

In order to determine if differences in metal ion selectivity are due to changes in the microenvironment, bifunctional IPNs have been prepared with imidazole groups whose microenvironment is varied by copolymerizing vinylimidazole with different levels of ethyl acrylate. As was discussed with the molecular-recognition studies, the ethyl acrylate alters the polarity of the microenvironment of the resin. The imidazole's affinity for Cu(II) and Co(II) is quantified with binding constants as a function of the imidazole/ester ratio. Also investigated were the ion-

exchange/coordination capabilities of a series of IPNs consisting of carboxylic acid and imidazole ligands which were contacted with Cu(II), Co(II), Zn(II), Ni(II), and Cd(II). Again, all interactions were quantified with binding constants, K_{11}, which are described in detail in the Appendix.

A shortcoming of coordinating and ion exchange resins can be the slow uptake of metal ions due to steric hindrance of the dense polymeric matrix. For this reason, initial ionic recognition studies were conducted with a 24 hour contact period, but after a kinetic study, all additional studies utilized a 7 day contact period. Seven days were needed for the more concentrated metal ion solutions to equilibrate with the IPNs.

Hard-soft acid-base (HSAB) theory was used to predict the affinity of the ligands for the ionic substrates. HSAB theory states that hard acids prefer to bind to hard bases and soft acids prefer to bind to soft bases. Lewis acids can be classified into categories of hard, borderline, or soft based upon physical properties such as polarizability, electronegativity, and oxidation potential. Hard metal ions generally have one or more of the following characteristics: small size, high positive charge, no easily distorted outer orbitals, high electronegativity, and low polarizability[73]. In contrast, soft metals tend to be large in size, have low positive charge and contain unshared electrons in their valence shell which leads to high polarizability of the orbitals and low electronegativity[73]. The coordinating ligand, imidazole, is considered hard (the N is sp^2 hybridized), and it would be expected to bind more strongly to hard metals.

Initial Ionic Recognition Studies

Initial recognition studies investigated the complexing of the imidazole IPN, the 50% VIm-50% EA IPN (VIm-EA), and the hydrolyzed 50% VIm-50% EA IPN (VIm-AA), with Cu(II) and Co(II). The metal ion affinities were measured from solutions of $Cu(NO_3)_2$ and $Co(NO_3)_2$, each buffered to pH 5 with 0.6 N sodium acetate/acetic acid. The buffer was used to keep the pH constant. The IPNs were pre-equilibrated with the acetate buffer prior to contact with the Cu(II) or Co(II) solutions. Then, 1 meq of resin was contacted with 10 mL of the approriate solution. The normality of the solutions varied according to the R_i (R_i = meq of metal ion/meq of IPN). After contacting 24 hours, the solutions were analyzed by atomic absorption spectrometry, and the complexation data were determined for the adsorption isotherms.

The r vs. c curve for the IPNs binding Cu(II) and the *y*-reciprocal plot are shown in Figure 23 and Figure 24, respectively, and the saturation capacity, S_t, and the binding constant, K_{11}, for each interaction is in Table 13. The linearity of the *y*-reciprocal plots indicate 1:1 complex formation. The K_{11} values for the VIm, VIm-EA, and VIm-AA IPNs are 617, 257, and 252 N^{-1}, respectively. The VIm-EA IPN has a much lower Cu(II) S_t (0.6 meq/g), but a binding constant that is almost identical (257 N^{-1}) to the VIm-AA IPN. The K_{11}'s for Co(II) are 99, 181, and 76 N^{-1} for the order listed above. The S_t's for the VIm and the VIm-AA are approximately the same as with Cu(II), but the VIm-EA increased to 1.5. Also, the VIm-EA has the strongest interaction with Co(II).

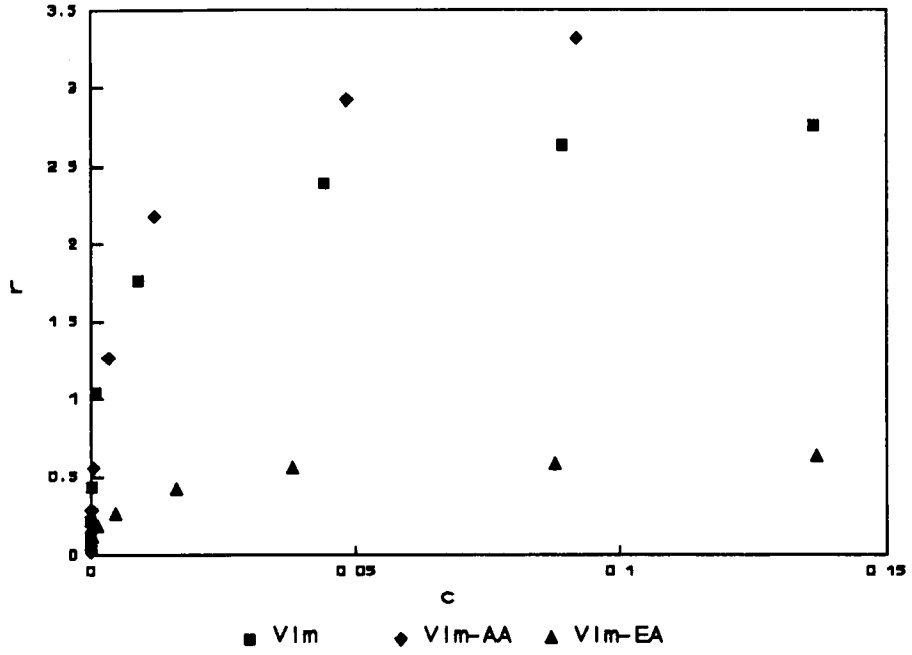


Figure 23. Adsorption Isotherms of IPNs with Cu(II).

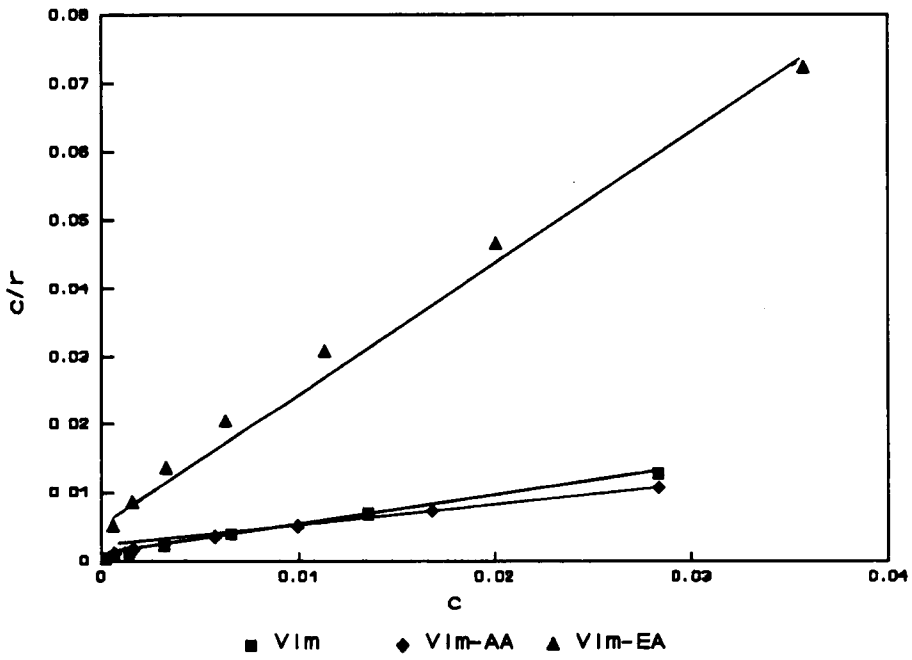


Figure 24. *y*-Reciprocal Plot of IPNs with Cu(II).

Table 13. K_{11}'s of Imidazole-Based IPNs with Cu(II) and Co(II) after 24 Hour Contact.

	Cu		Co	
IPN	S_t	K_{11} (N^{-1})	S_t	K_{11} (N^{-1})
VIm	2.8	617	2.9	99
VIm-EA	0.6	257	1.5	181
VIm-AA	3.3	252	2.9	76

The imidazole IPN displays quite different ion binding behavior compared to the bifunctional IPNs. Additionally, the imidazole IPN binds Cu(II) more strongly than Co(II) in spite of an identical saturation capacity for the two ions. The bifunctional IPN microenvironment is different from the monofunctional IPN: the Cu(II) K_{11} for the VIm-AA IPN is 252 N^{-1} compared to 617 N^{-1} for the VIm IPN. This would suggest that the imidazole and acid ligands are proximate enough within the IPN to form a different environment for binding to the metal ion. The lower K_{11} value for the VIm-AA IPN is due to the polarity of the acid ligand, rather than to inter-ligand hydrogen bonding, since the VIm-EA IPN gives an almost identical binding constant.

The IPN binding constants are consistent with what would be expected from the soluble analogues[74,75]. Acetic acid has a first formation constant of 51 N^{-1} with Cu(II) and 6.5 N^{-1} for Co(II) from solutions with an ionic strength of 1 N. The corresponding values for imidazole are 21,400 N^{-1} and 263 N^{-1} for copper and cobalt, respectively, from 0.16 N ionic strength solutions.

Ionic Recognition with Polystyrene/Poly(vinyl imidazole-co-ethyl acrylate) IPNs

The effect of the microenvironment surrounding the imidazole ligand within an IPN on metal ion binding was examined and quantified with binding constants. The microenvironment was varied as increasing levels of imidazole were replaced with weakly coordinating ester groups. The metals examined include Cu(II) and Co(II) in a

pH 5 acetate buffer solution with the same procedure as discussed for the initial ionic recognition studies. One notable difference from the earlier procedure was that the contact time was extended from 24 hours to 7 days to ensure equilibrium. A kinetic study found that the more dilute solutions equilibrated rapidly, while the more concentrated solutions could take up to 6 days; as a result all vials were shaken for 7 days.

The IPNs examined contain 100%, 77%, 53%, 27%, and 0% VIm (the last thus being pure ester IPN). The adsorption isotherm and *y*-reciprocal plot of the IPNs with Cu(II) are shown in Figures 25 and 26, respectively. The same graphs of the complexation of Co(II) with the IPNs are displayed in Figures 27 and 28. The corresponding Cu(II) and Co(II) binding constants and saturation capacities are shown in Table 14.

For all imidazole-containing IPNs, there is a much greater affinity for Cu(II) than for Co(II). The microenvironment within the IPN having an equimolar mix of imidazole and ester sites is sufficiently different from the other IPNs that it binds copper most strongly. The Cu affinity changes are accompanied by a continuous decrease in the saturation capacity, which is greater than can be explained by the decrease in the imidazole content. The imidazole-Co(II) affinity is low and remains low as the microenvironment is varied. The highest Co(II) saturation capacities are lower than those with Cu(II). The ester IPN does not bind Cu(II) or Co(II).

As discussed earlier, the microenvironment of the IPNs changes as the imidazole/ester ratio changes which was demonstrated with swelling ratios in methanol

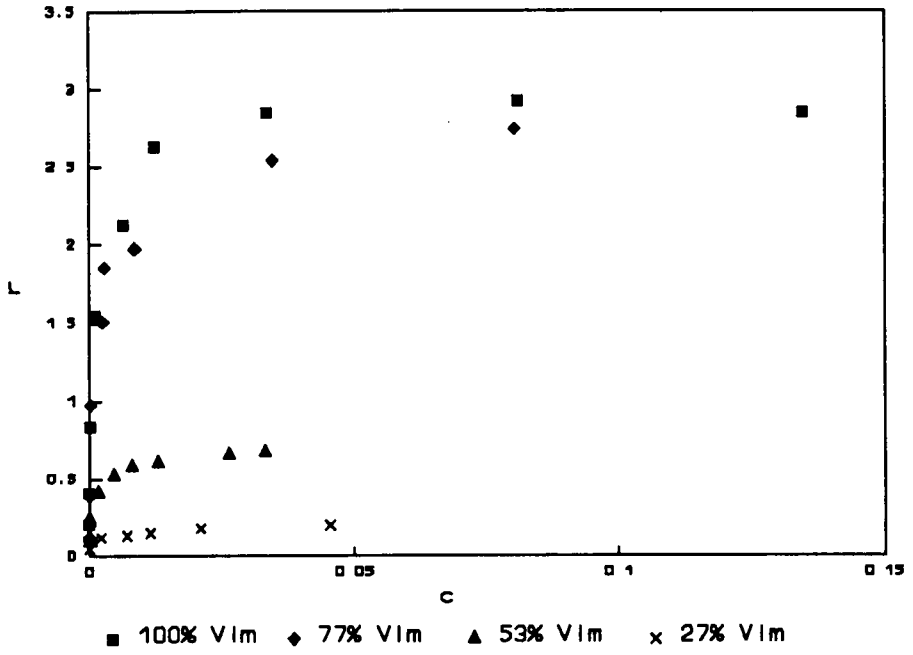


Figure 25. Adsorption Isotherm of VIm-EA IPNs with Cu(II).

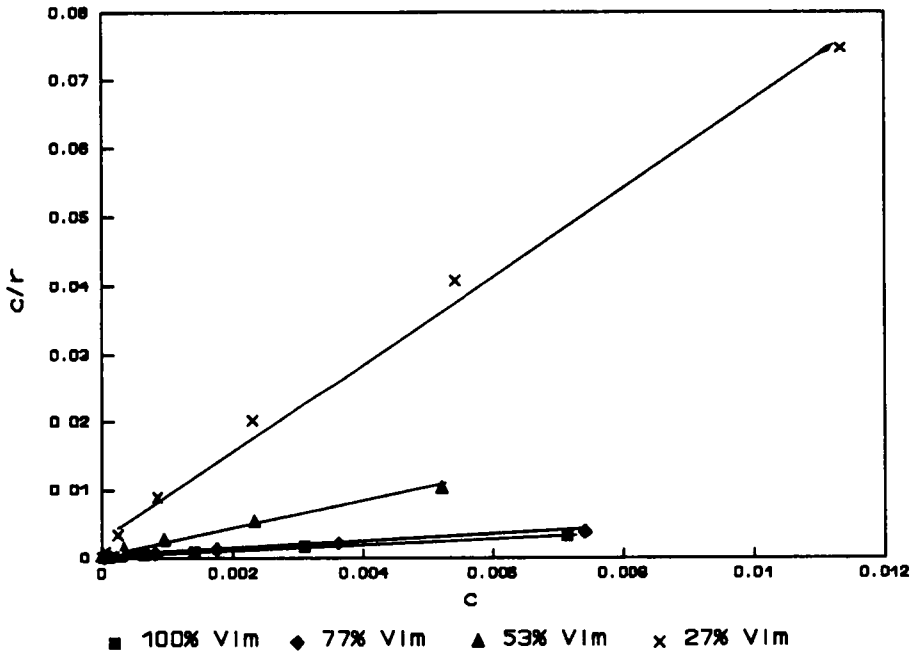


Figure 26. *y*-Reciprocal Plot of VIm-EA IPNs with Cu(II).

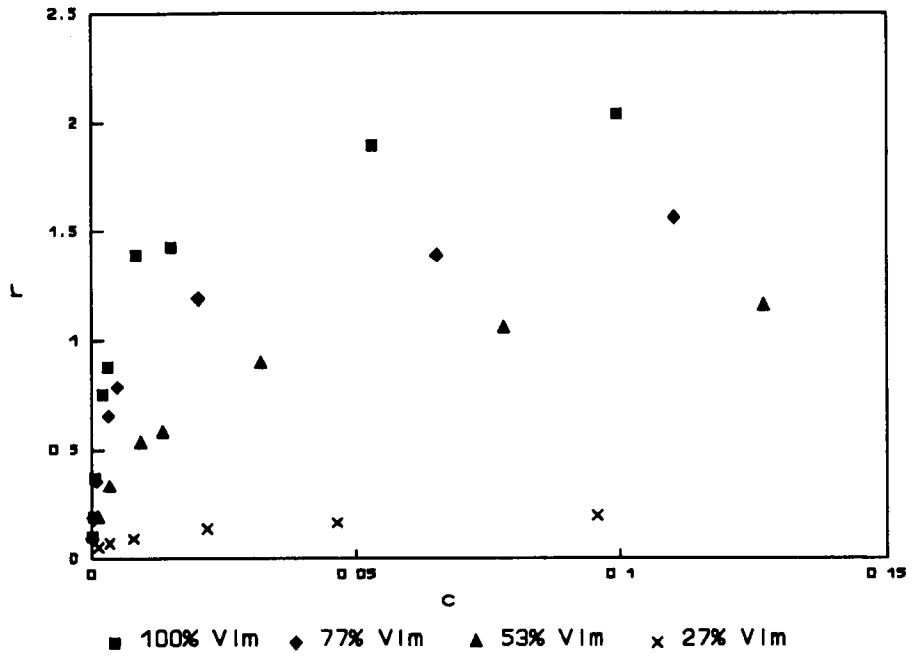


Figure 27. Adsorption Isotherm of VIm-EA IPNs with Co(II).

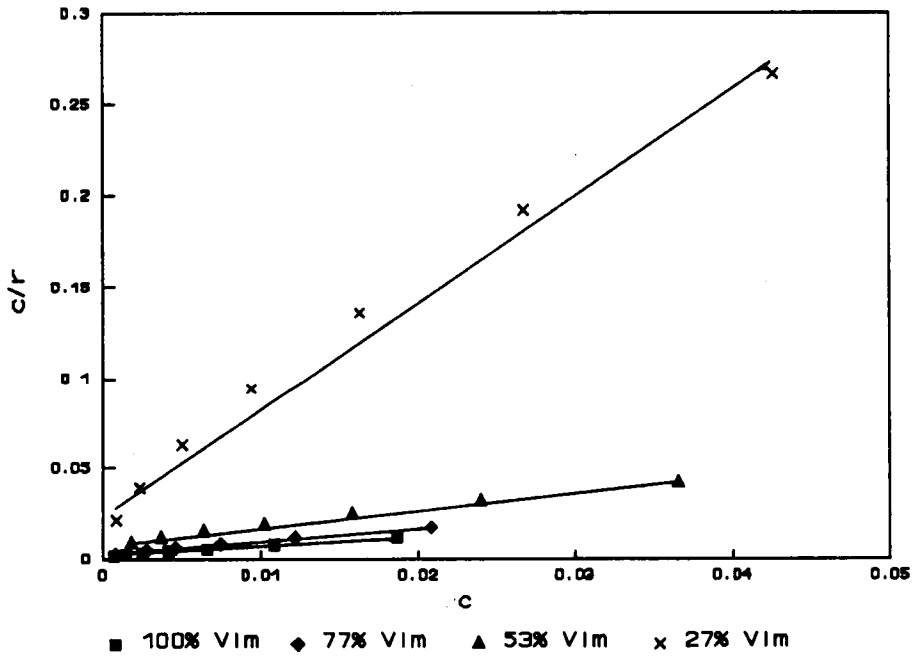


Figure 28. *y*-Reciprocal Plot of VIm-EA IPNs with Co(II).

Table 14. K_{11}'s of VIm-EA IPNs with Cu(II) and Co(II).

	Cu(II)		Co(II)	
Imidazole (%)	S_t	$K_{11}(N^{-1})$	S_t	$K_{11}(N^{-1})$
100%	2.8	2761	1.8	324
77%	2.5	2589	1.5	296
53%	0.6	6757	1.1	117
27%	0.2	2800	0.2	188
0%	0	0	0	0

and 1,4-dioxane. The 100% imidazole IPN had the greatest swelling ratio in the more polar solvent methanol and hence, the more polar microenvironment. Similarly, the ester IPN had the greatest swelling ratio in the 1,4-dioxane and has the least polar microenvironment.

The monofunctional IPNs show that Cu(II) binds strongly to imidazole and has no affinity for carboxylate esters. Changing from 100% to 77% VIm does not affect the Cu(II) K_{11} which indicates that both IPNs have a comparable environment and is supported by identical swelling ratios in 1,4-dioxane (1.00). The 27% VIm IPN complexes only 0.2 mequiv Cu(II) with the same binding constant as the imidazole IPN. This is consistent with surface complexation of the Cu(II) where microenvironmental differences are minimized. The equimolar imidazole:ester IPN is unique in that it binds the Cu(II) more strongly than expected from results with the 100% imidazole IPN.

A microenvironmental effect in which the polar ester groups increase the strength of the imidazole-Cu interaction could be evident. In this case, the acetate ion is brought into the polymer matrix along with the copper ion in order to maintain electroneutrality. $Cu(OAc)_2$ has a higher formation constant than $Cu(NO_3)_2$ [74]. Since the anion can influence the selectivity displayed by a molecule when coordination is the sole mechanism of complexation[76], it is possible that the acetate moiety is more compatible with the less polar environment of the VIm-ester IPN as the ester content increases to an equimolar level with the imidazole. As the ester content continues to increase, the polarity of the microenvironment decreases to the point where metal

complex formation is unfavorable. This also accounts for the low saturation capacity displayed by the 27% VIm IPN.

The imidazole-Co affinity is low with all IPNs studied. Again, this is consistent with the soluble analogues[74,75]. Imidazole has a first formation constant of 21,400 N^{-1} with Cu(II) and 263 N^{-1} with Co(II) in solutions of 0.16 N ionic strength.

Ionic Recognition Studies with Hydrolyzed Polystyrene/Poly(vinyl imidazole-co-ethyl acrylate) IPNs

A series of IPNs containing different ratios of imidazole to carboxylic acid ligands (obtained by hydrolysis of the ester group) were investigated and the effect of the microenvironment on metal ion binding was quantified. The IPNs consisted of 100%, 76%, 53%, and 27% VIm and an IPN that was solely hydrolyzed ester ligands or carboxylic acid (AA). The metals examined include Co(II), Ni(II), Cu(II), Zn(II), and Cd(II). All of the IPNs were contacted with the Co(II) and Cu(II); however, only the 100% VIm, 53% VIm-AA, and 100% AA were contacted with Ni(II), Cd(II), and Zn(II). The procedure followed that of the VIm-EA ionic- recognition studies.

Adsorption isotherms of the 100% VIm, 53% VIm-AA, and 100% AA IPNs with Cu(II), Co(II), and Cd(II) are shown in Figures 29, 31, and 33, respectively. The corresponding y-reciprocal plots are shown in Figures 30, 32, and 34 for the metals listed above. The binding constants and saturation capacitities for all metal ions and IPNs are displayed in Table 15.

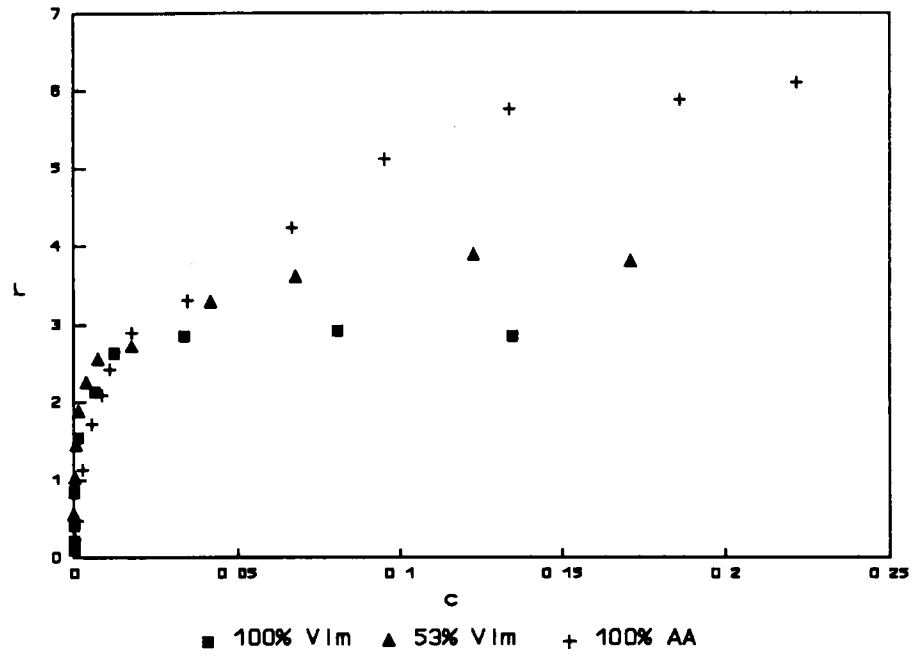


Figure 29. Adsorption Isotherm of VIm-AA IPNs with Cu(II).

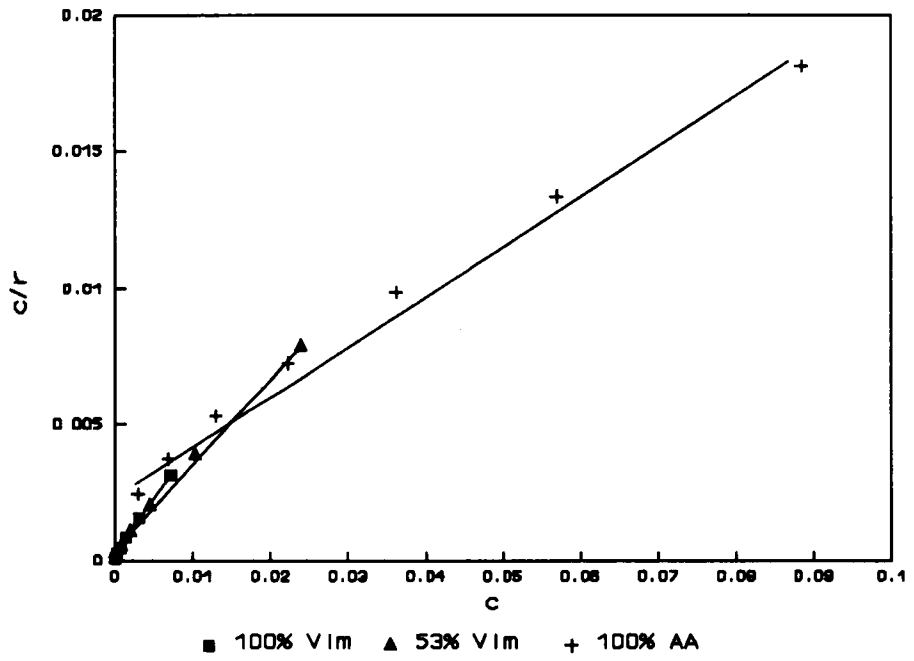


Figure 30. *y*-Reciprocal Plots of VIm-AA IPNs with Cu(II).

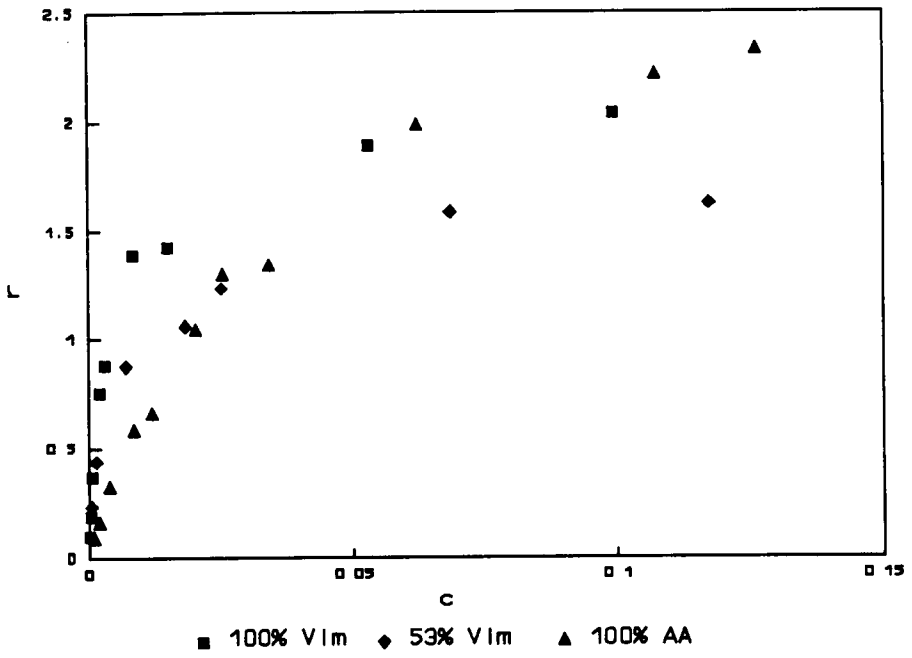


Figure 31. Adsorption Isotherms of VIm-AA IPNs with Co(II).

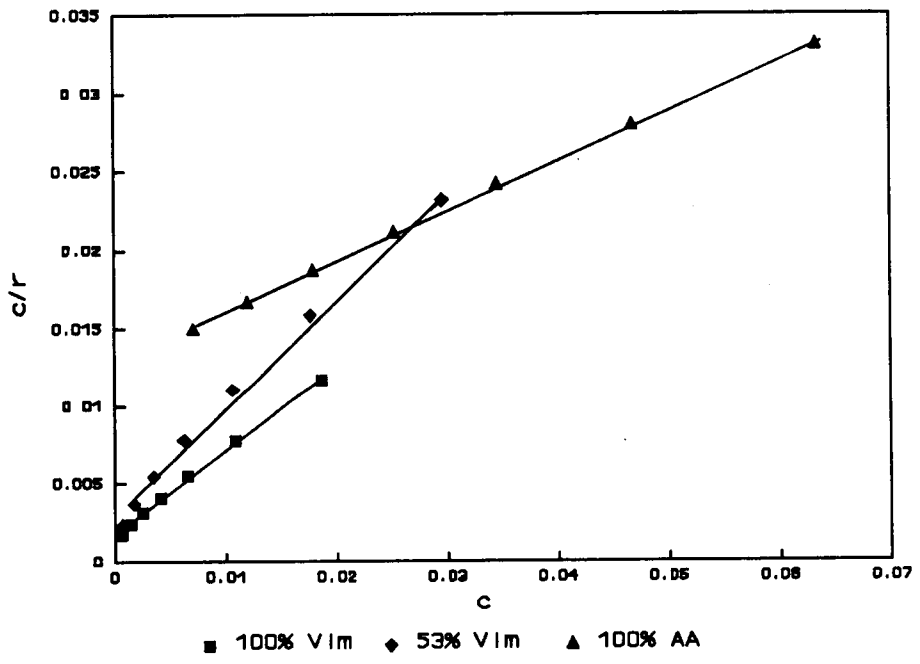


Figure 32. *y*-Reciprocal Plots of VIm-AA IPNs with Co(II).

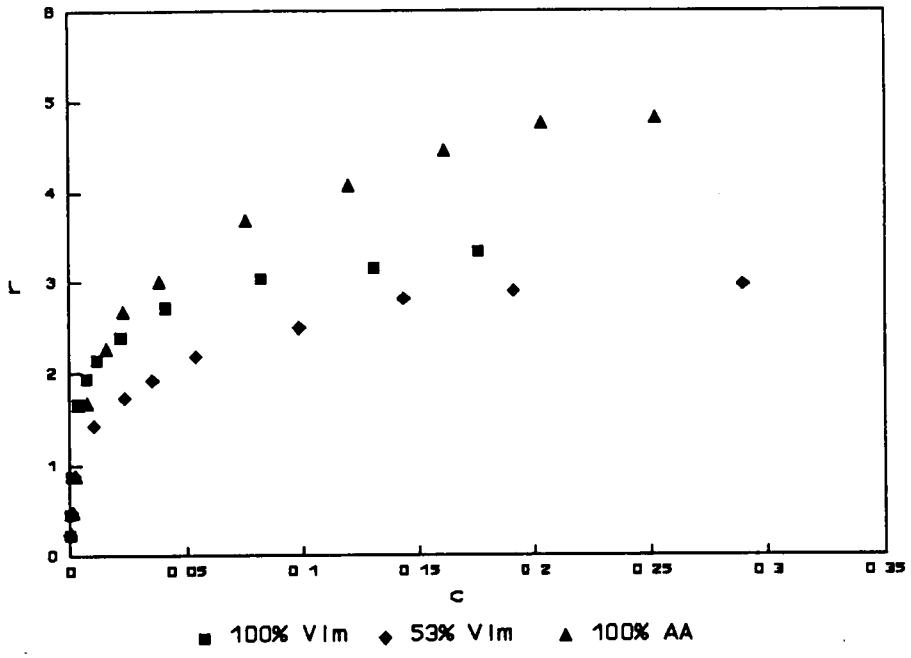


Figure 33. Adsorption Isotherms of VIm-AA IPNs with Cd(II).

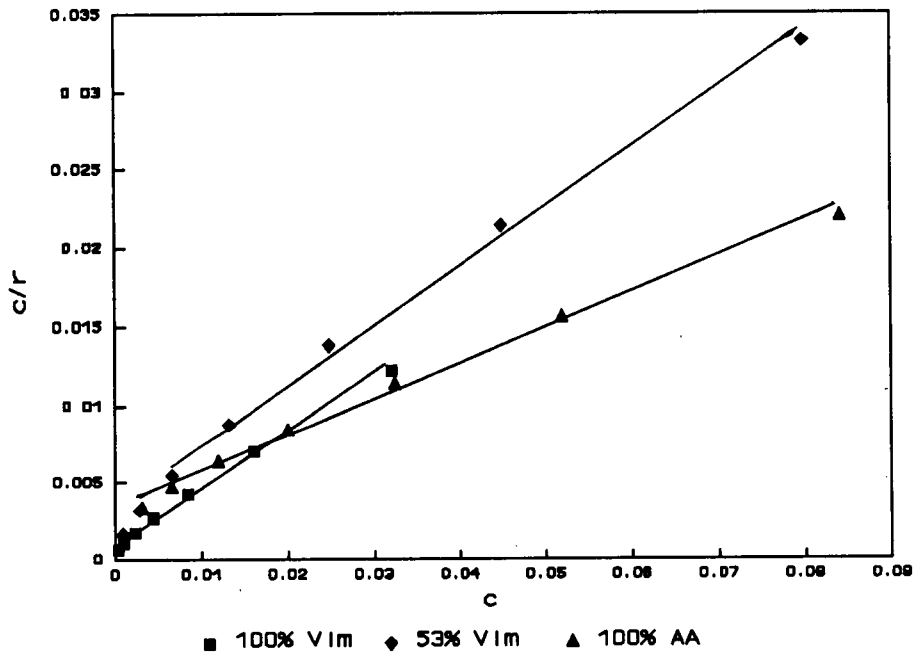


Figure 34. *y*-Reciprocal Plots of VIm-AA IPNs with Cd(II).

Table 15. K_{11}'s of VIm-AA IPNs with Metal Ions.

	Co(II)		Ni(II)		Cu(II)		Zn(II)		Cd(II)	
IPN	S_t	K_{11}	S_t	K_{11}	S_t	K_{11}	S_t	K_{11}	S_t	K_{11}
100% VIm	1.8	324	2.8	846	2.9	2761	3.4	2671	3.3	413
76% VIm	1.6	280			2.2	3081				
53% VIm	1.6	256	2.3	325	3.8	1099	3.2	527	3.0	145
27% VIm	1.4	184			3.2	718				
100% AA	2.4	25	3.5	19	6.1	65	3.6	37	4.8	69

For all imidazole-containing IPNs, the binding to Cu(II) is stronger and the saturation capacity is greater than with any other metal ion examined. The 76% VIm-AA IPN has the greatest binding constant to Cu(II) which is only 10% greater than the 100% VIm-Cu(II) K_{11} (also, a 15% difference with Co(II)); this indicates that both IPNs have similar microenvironments which is consistent with earlier conclusions concerning the 100% VIm and 77% VIm-ester IPNs. As the imidazole content decreases and the carboxylic acid ligands increase, a greater percentage difference in K_{11}'s was observed with Cu(II) than with Co(II). Therefore, the Cu(II) binding is more sensitive to changes in the microenvironment than Co(II). The 100% AA IPN consistently has the highest S_t and the lowest K_{11} for the metal ions; thus, a greater number of ions are complexed but are more loosely bound.

The results correspond well to HSAB theory. The imidazole nitrogen that coordinates is hard and binds more strongly to the harder metals Cu(II) and Zn(II). The softer metal ions, Co(II) and Cd(II), have the lowest binding constants with the VIm IPN. The experimental results also correspond well to the first formation constants of the small molecule analogues[74,75]. Acetic acid has first formation constants in the increasing order of Co(II) < Ni(II) < Zn(II) < Cd(II) < Cu(II), while the AA IPN demonstrates increasing binding strength in the order of Ni(II) < Co(II) < Zn(II) < Cu(II) < Cd(II). Similarly, imidazole has first formation constants in the increasing order of Co(II) < Cd(II) < Zn(II) < Ni(II) < Cu(II), while the VIm IPN shows increasing binding strength in the order of Co(II) < Cd(II) < Ni(II) < Zn(II) < Cu(II).

Conclusions

Ionic recognition studies indicate that the ligand-metal ion interactions are affected by the polymeric microenvironment. The metal ion selectivities displayed by bifunctional polymers are dependent on cooperative effects between the different ligands and a superimposed microenvironmental effect. The corresponding monofunctional polymers must be studied so as to set a baseline against which the performance of the bifunctional polymers can be evaluated. Ligands used to interact with substrates should be sterically similar to those used to vary the microenvironment in order to identify cooperating ligand interactions. Methyl or ethyl ester groups that can be hydrolyzed to free acid sites are an important example of this pairing.

CHAPTER V

EXPERIMENTAL PROCEDURES

Xerogel Polystyrene Synthesis

Xerogel[58] polystyrene beads were prepared by the technique of suspension polymerization. The first part of the aqueous phase contained 0.96 g of gelatin (serves as stabilizer to keep the monomer droplets from agglomerating during the polymerization) dissolved in 100 g of water which was heated to 50 °C. This was added to the second part of the aqueous phase which was composed of 11.90 g of poly(diallydimethylammonium chloride) (a suspending agent; it increases the viscosity of the aqueous phase) and 0.65 g of boric acid (a buffer) in 216.5 g of water adjusted to pH 10.0 (using 50% NaOH). The two parts were combined, and the pH was readjusted to 10.0 using 50% NaOH to prevent the decomposition of the gelatin. The aqueous phase was added to a suspension polymerization apparatus that was comprised of a 1 L three-necked roundbottom flask equipped with a condenser, a thermometer to which a temperature controller was attached (Thermowatch, Instruments for Industry and Research), and a constant-torque overhead stirrer (Con-Torque, Eberach Co.) with a double-paddled stainless-steel stirrer. Before addition of solutions to the

roundbottom flask, the stir motor was adjusted to 350 rpm (by using a Biddle dial tachometer) to give predominantly -40 + 60 mesh beads. Oxygen was excluded from the system by a nitrogen purge, which was begun at least 30 minutes before the addition of the aqueous phase and continued throughout the reaction.

To prepare a 2% crosslink level gel copolymer, the organic phase consisted of 171.7 g styrene (Aldrich Chemical Co.), 6.50 g divinylbenzene (corrected for 44.6% ethylstyrene, Dow Chemical Co.), 120.0 g of toluene (40 wt % of organic phase, Aldrich Chemical Co.), and 1.80 g of benzoyl peroxide (Aldrich Chemical Co.) as the initiator. The toluene was used to give larger micropores. After the addition of the organic phase to the reaction flask, the proper suspension was obtained by the use of three cycles of two minutes stir and one minute settle period. The reaction was heated to 80 °C over a two-hour period (7 °C every 15 minutes) and held at 80 °C for 10 hours. The reaction mixture was then heated to 94 °C (reflux) for 2 hours to ensure complete polymerization. After cooling to room temperature, the beads were washed with aqueous HCl at pH 4 twice and methanol twice. Each wash was accompanied by a 15 minute stir period. After all of the methanol was removed, the polystyrene required soxhlet extraction with toluene for 17 hours to remove unreacted monomer, oligomers, and toluene from the beads. The beads were then dried at 60 °C overnight and sieved the following day.

Dimethylamine Resin Synthesis

A 250 mL three-necked roundbottom flask was equipped with a condenser (with a balloon fastened to the end), a thermometer, and an overhead stirrer. Ten grams of poly(vinylbenzyl chloride) beads and 100 mL 40% aqueous dimethylamine solution (Aldrich Chemical Co.) were added to the flask and heated to reflux. The temperature was maintained for 17 hours. After cooling to room temperature, the beads were placed in a fritted glass funnel and conditioned using the sequence (1L/1 hour): H_2O, 4 wt % HCl, H_2O, 4 wt % NaOH, H_2O. The resin was then analyzed for % solids, TAEC, and SSAC.

Interpenetrating Polymer Network Synthesis

The synthesis of a 100% vinyl imidizole IPN will be described. A monomer solution containing 24.00 g N-vinylimidizole (0.2550 moles, Aldrich Chemical Co.), 7.34 g divinylbenzene (10 mole %, corrected for 44.6% ethylstyrene impurity; Dow Chemical Co.), and 1.13 g AIBN [azobis(isobutyronitrile); Polysciences] was stirred in a graduated cylinder and then brought to a total volume of 60 mL with toluene (Aldrich Chemical Co.) to make the solution 4.25 M in functional monomer. The monomer solution was sparged with nitrogen for 5 minutes and then allowed to swell with 10 g of polystyrene beads 1.5 hours.

A suspension polymerization apparatus consisting of a 250 mL three-necked roundbottom flask equippped with a condenser, thermometer to which a temperature

controller was attached (Thermowatch, Instruments for Industry and Research), and overhead stirrer with single-paddle stirrer was utilized. The aqueous phase was 1.5 wt % polyvinylalcohol based on monomer weight and 41.7 g calcium chloride dihydrate per 80 mL of aqueous solution. For 10 g of beads, 134.28 g of aqueous phase was needed; therefore, 160 mL of aqueous solution was made. With this N-vinylimidazole IPN, 0.90 g of polyvinylalcohol (Fluka Chemical Co.) were dissolved in 80 mL of water and then, 83.4 g of calcium chloride (dihydrate, Aldrich Chemical Co.) was added and stirred. The solution was brought to a total volume of 160 mL with water and stirred again. 134.28 g of the aqueous phase was placed in the reaction flask and heated to 80 °C. The beads were filtered for 5 minutes, and the monomer solution that was removed was collected and measured. Next, the beads were placed in the hot aqueous phase while heating and stirring continued. The polymerization runs for 12 hours at 80° C.

After polymerizing, the beads were washed 4 times with hot water to remove the aqueous phase and underwent soxhlet extraction with methanol for 17 hours. The beads were placed in a fritted glass funnel and conditioned with the sequence: water, 4 wt % NaOH, water, 4 wt % HCl, water. The beads were characterized by acid capacity, base capacity, percent solids, and TAEC.

The amount of monomer solution needed varied with the amount of beads used and the type of monomer present in the greatest amount.

Acid Hydrolysis

Approximately 5 g of Buchner-dried beads and a few boiling chips were placed in a 250 mL roundbottom flask which was equipped with a condensor. 200 mL of 12 N HCl were added, and the mixture was heated to reflux. The temperature was maintained for 56 hours. For larger amounts of beads (10-20 g), 400 mL of 12 N HCl were used, and the solution was relplaced after 24 hours.

Base Hydrolysis

Approximately 5 g of Buchner-dried beads, a few boiling chips, and 250 mL of a 2 N KOH (in aqueous dioxane) solution were placed in a 250 mL roundbottom flask equipped with a condenser. The mixture refluxed for 56 hours. If 10 g to 20 g of beads were to be hydrolyzed, 500 mL of 2 N KOH (in aqueous dioxane) were used, and the solution was replaced after 24 hours.

Determination of Percent Solids

The conditioned resin was suction-dried at 720 mm Hg for 5 minutes, with the Buchner funnel covered by a rubber sheet held in place with a rubber band. Approximately 1 g of accurately weighed resin was then placed in an oven at 110 °C

for 17 hours. The resin was allowed to cool in a desiccator and then reweighed. The % solids was calculated according to the following equation:

$$\%\ solids = \frac{oven\text{-}dried\ resin\ wt}{buchner\text{-}dried\ resin\ wt} \times 100\%$$

Determination of Acid Capacity

Approximately 0.5 to 1.0 g of Buchner-dried resin was placed in a 250 mL Erlenmeyer flask with a ground glass joint and stirred for 17 hours with 200 mL standard 0.1 N NaOH which was 5 wt % NaCl. A 50 mL aliquot of the NaOH solution was titrated with 0.1 to 0.15 N H_2SO_4 using phenolphthalein as the indicator. The acid capacity, which is accurate to $\pm$ 0.2 mequiv/g, was calculated using the following equation:

$$Acid\ Capacity = \frac{(vol\ NaOH)\ (N\ NaOH) - 4\,(vol\ H_2SO_4)\ (N\ H_2SO_4)}{grams\ of\ dry\ resin}$$

The weight of dry resin was determined by multiplying the buchner-dried resin by the percent solids. The NaOH solution is standardized against primary standard potassium hydrogen phthalate and subsequently used to standardize the H_2SO_4 solution.

Determination of Base Capacity

The same procedure that was utilized to determine acid capacity was followed except that 0.1 N acid was stirred with the beads and the titration was completed with 0.1 N base.

Determination of Total Anion-Exchange Capacity (TAEC)

A 5-10 g buchner-dried sample of resin containing the amine functional group was placed in a fritted glass funnel, converted to the chloride form by elution with HCl, and eluted with 1 L of 1 N $NaNO_3$ for 1 hour, with the effluent being collected in a 1 L volumetric flask. A 50 mL aliquot of this solution was placed in a 250 mL Erlenmeyer flask, acidified with concentrated HNO_3 to a methyl orange endpoint (red), and neutralized with 0.3 N NaOH (yellow). A Mohr titration was then performed to determine the amount of chloride present with standard 0.05 N $AgNO_3$ employing 2 mL of an aqueous 5 wt % K_2CrO_4 indicator. The TAEC was calculated using the equation:

$$TAEC = \frac{20\ (Vol\ AgNO_3)\ (N\ AgNO_3)}{grams\ dry\ resin}$$

Determination of Salt Splitting Anion-Exchange Capacity (SSAC)

Approximately 5-10 g of a buchner-dried sample was placed in a fritted glass funnel, and 1 L of 4 wt % NaOH, 1 L H_2O, and 1 L 1 N $NaNO_3$, were eluted (1 L/1 hour). The effluent was collected in a 1L volumetric flask. A 50ml aliquot was then titrated with standard H_2SO_4. The SSAC is equivalent to the mequiv OH^-, which were the associated counterions to the quatermary amine sites, displaced by the NO_3^- per dry gram of resin which was calculated by the equation:

$$SSAC = \frac{20\ (Vol\ H_2SO_4)\ (N\ H_2SO_4)}{grams\ dry\ resin}$$

Molecular-Recognition Studies

A molecular-recognition study with a dimethylamine resin contacted with benzoic acid will be described as an example of the experimental procedure for molecular recognition. A series of benzoic acid solutions in methanol with the appropriate concentrations were obtained. For example, the sample at an R_i of 1.0 would require a benzoic acid solution of 0.1 N. One mequiv of resin was accurately weighed into each container. Approximately 15 mL of methanol were added to each

bottle, which was shaken for 15 minutes. The methanol was gently removed so that no beads were lost. This process was repeated three more times.

After the last solvent exchange, the methanol was removed, and the residual methanol in the bottle was allowed to evaporate for a few minutes. Next, a stir bar and 10 mL of the appropriate contact solution were added to each sample. The samples were stirred 17 hours at 350 rpm. The same results were obtained by shaking the samples for the same amount of time.

When the contact time was completed, each sample was poured into a centrifuge tube and sealed with a rubber stopper (the beads may be crushed). The tubes were placed in the centrifuge for 10 minutes at 2000 rpm. After the samples were centrifuged, 5 mL of contacted solution were titrated with NaOH using phenolphthalein indicator. Also, 5 mL of the standard solution (acid before contact) were titrated by the same base, and the percent complexed by the resin was calculated by the equation:

$$\%\,Cmpl = 1 - \frac{vol.\ NaOH\ req.\ for\ titrating\ contacted\ sol.}{vol.\ NaOH\ req.\ for\ titrating\ standard\ sol.} \times 100\%$$

To ensure accuracy, the concentration of the base did not exceed the concentration of the standard acid, and a 10 mL buret was used for the samples with dilute concentrations.

Ionic Recognition Studies

All ionic recognition studies were completed at pH 5 using 0.6 N acetic acid/sodium acetate buffer. The contact solutions were made in 100 mL quantities. The appropriate amount of metal nitrate salt was placed in a beaker with 20 mL of 3 N acetic acid, and a quantity of water was added to give 80 mL. The solution was adjusted to pH 5 with NaOH and quantitatively transferred to a 100 mL volumetric flask. The solution was mixed and stored in a plastic bottle.

An accuratedly weighed sample of Buchner-dried resin containing 1 mequiv of active sites was placed in a 20 mL scintillation vial. The resin underwent solvent exchange by shaking four times (15 min) with approximately 15 ml of 0.6 N acetate buffer at pH 5. After the final solvent exchange and removal of the buffer, 10 mL of the appropriate contact solution were added, and the samples were shaken for 7 days.

After the contact had been completed, the final pH of the solution was measured. A portion of the sample was then diluted (with 0.6 N acetate buffer to keep the matrix constant) to a concentration which was within the linear range of the atomic absorption spectrophotomter (Varian AA-1475) for that metal. The concentration of the contacted solution was then determined from the AA and the following equation:

$$\%\ Abs = \frac{(N\ standard\ soln) - (N\ contacted\ soln)}{N\ standard\ soln} \times 100\%$$

Determination of Purity of Metal Salts

Copper

A solution of 15 mg of copper(II) nitrate in 100 mL of water was obtained, and the pH was adjusted to about 8 with 1 M ammonium hydroxide. Ten mL of ammonium chloride was added to ensure that the ammonia did not produce too high a pH. Murexide was added, and the titration with EDTA was completed with a color change from yellow to violet at the endpoint.

Cobalt

A solution of 20 mg of cobalt nitrate in 100 mL of water was examined. Murexide was added to the solution, and it turned an orange yellow color. The cobalt-murexide complex now served directly as an acid-base indicator for further neutralization in which ammonia is added until the color changes to yellow. Titration with EDTA was then completed until a sharp color change from yellow to violet.

Zinc

A 100 mL solution containing 25 mg of zinc nitrate was neutralized with sodium hydroxide until a pH of 7 was reached. Two mL of pH 10 buffer (ammonium chloride and ammonium hydroxide) were added, and then, the indicator Erio T was added to give the solution a purple-red color. The sample was titrated with 0.01 M EDTA to a blue endpoint.

Nickel

A 100 mL sample containing 15 mg of cadmium nitrate was neutralized with sodium hydroxide, and then murexide was added. Ten mL of ammonium chloride was added, and if the solution turned orange-yellow, a few drops of concentrated ammonium hydroxide were added. The solution was titrated with 0.01 M EDTA, and just before the endpoint, 10 mL of concentrated ammonium hydroxide were added. The endpoint was reached when the solution changed from yellow to violet.

Cadmium

The analysis for cadmium nitrate followed the zinc procedure except that only 0.5 mL of pH 10 buffer was used.

LIST OF REFERENCES

1. Adams, B. A.; Holmes, E. L. *J. Soc. Chem. Ind.* (London) **1935**, *54*, 1T.

2. *Polymeric Reagents and Catalysts*; Ford, W. T., Ed.; American Chemical Society: Washington, D. C., **1986**.

3. *Synthesis and Separations Using Functional Polymers*; Sherrington, D. C.; Hodge, P., Eds.; John Wiley: New York, **1988**.

4. Arshady, R.; Ledwith, A. *Reactive Polymers* **1983**, *1*, 159.

5. Munzer, M.; Trommsdorff, E. *High Polymers* **1977**, *29*, 106.

6. Jacobelli, H.; Bartholin, M.; Guyot, A. *J. Appl. Polym. Sci.* **1979**, *23*, 927.

7. *Polymer-Supported Reactions in Organic Synthesis*; Hodge, P.; Sherrington, D. C., Eds.; John Wiley: New York, *1980*.

8. Helfferich, F. *Ion Exchange*; McGraw-Hill: New York, **1962**.

9. Hodge, P. *Chem. Brit.* **1978**, *14*, 237.

10. Michelo, R.; Heitz, W. *Makromol. Chem.* **1975**, *176*, 245.

11. Frechet, J.; Warock, J.; Farrall, M. *J. Org. Chem.* **1978**, *43*, 2618.

12. Frechet, J.; Darling, P.; Farrall, M. *J. Org. Chem.* **1981**, *46*, 1728.

13. Cardillo, G.; Orena, M.; Sandri, S. *Tetrahedron Lett.* **1976**, *17*, 3985.

14. Arrad, O.; Sasson, Y. *J. Org. Chem.* **1989**, *54*, 4993.

15. D'Alelio, G. F. U. S. Patent 2 340 111, 1944.

16. *Ion Exchange and Solvent Extraction*; Marinsky, J. A.; Marcus, Y., Eds.; Marcel Dekker: New York, 1973.

17. Dorfner, K. *Ion Exchangers: Properties and Applications*; Ann Arbor Science: Ann Arbor, 1972.

18. Albright, R. L.; Yarnell, P. A. In *Encyclopedia of Polymer Science and Engineering, 2nd Ed.*; Mark, H.; Bekales, N.; Overberger, C.; Menges, G., Eds.; John Wiley: New York, 1987; Vol. 8, p 341.

19. *Handbook of Ion Exchange Resins*; Korkisch, J., Ed.; CRC Press: Boca Raton, 1989.

20. Sahni, S.; Reedjk, J. *Coord. Chem. Rev.* **1984**, *59*, 1.

21. Strauss, S. D. *Power* **1984**, *128*, 18.

22. Alexandratos, S. D.; Strand, M. A.; Quillen, D. R.; Walder, A. J.; *Macromolecules* **1985**, *18*, 829.

23. Alexandratos, S. D.; Wilson, D. L.;Strand, M. A.; Quillen, D. R.; Walder, A. J. *Macromolecules* **1985**, *18*, 835.

24. Helfferich, F. In *Ion Exchange*; Marinsky, J. A., Ed.; Marcel Dekker: New York, 1966; Vol. 1, Chapter 2.

25. Janauer, G. E.; Gibbons, R. E.; Bernier, W. E. In *Ion Exchange and Solvent Extraction*; Marinsky, J. A.; Marcus, Y., Eds.; Marcel Dekker: New York, 1985; Vol. 9, Chapter 2.

26. Alexandratos, S. D.; *Sep. Purif. Meth.* **1988**, *17*, 67.

27. Alexandratos, S. D.; Wilson, D. L. *Macromolecules* **1986**, *19*, 280.

28. Alexandratos, S. D.; Quillen,D. R.; Bates, M. E. *Macromolecules* **1987**, *20*, 1191.

29. Alexandratos, S. D.; Bates, M. E. *Macromolecules* **1988**, *21*, 2905.

30. Crick, D. W.; Alexandratos, S. D. Characterization of Bifunctional Interpenetrating Polymer Networks via Solid State ^{13}C NMR Spectroscopy, submitted for publication.

31. Sperling, L. H. *Interpenetrating Polymer Networks and Related Materials*; Plenum: New York, 1981.

32. Millar, J. R. *J. Chem. Soc.* **1960**, 1311.

33. *Encyclopedia of Polymer Science and Engineering, 2nd Ed.*; Mark, H. F.; Bikales, N. M.; Overburger, C. G.; Menges, G., Eds.; John Wiley: New York, 1987; Vol. 8, p 279.

34. Visscher, K. B.; Manners, I; Allcock, H. R. *Macromolecules* **1990**, *23*, 4885.

35. Frisch, H. L.; Zhou, P.; Frisch, K. C.; Xiao, X. H.; Huang, M. W.; Ghiradella, H. *J. Polym. Sci., Polym. Chem.* **1991**, *29*, 1031.

36. Lee, O. S.; Park, T. S. *Polym. Journal* **1991**, *23*, 241.

37. Abu-Isa, I. A. *J. Appl. Polym. Sci.* **1991**, *43*, 1133.

38. Acevedo, M.; de Abajo, J.; de la Campa, J. G. *Polymer* **1991**, *32*, 2210.

39. Kolarz, B. N. *Angew. Makromol. Chem.* **1980**, *90*, 167.

40. Kolarz, B. N. *Angew. Makromol. Chem.* **1980**, *90*, 183.

41. Barros, G. G.; Huang, M. W.; Frisch, H. L. *J. Appl. Polym. Sci.* **1992**, *44*, 255.

42. Huelck, V.; Thomas, D. A.; Sperling, L. H. *Macromolecules* **1972**, *5*, 340.

43. Frisch, H. L.; Huang, M. W. *J. Appl. Polym. Sci., Polym. Chem.* **1991**, *29*, 131.

44. Kelley, S. S.; Ward, T. C.; Glasser, W. G. *J. Appl. Polym. Sci.* **1990**, *41*, 2813.

45. Frisch, H. L.; Wang, L.; Huang, W.; Hua, Y. H.; Xiao, H. X.; Frisch, K. C. *J. Appl. Polym. Sci.* **1991**, *43*, 475.

46. Murthy, C. N.; Patni, M. J.; Deshpandte, D. D.; Kudchadker, A. P.; Mehta, M. H.; Ankleshwaria, B. V. *J. Appl. Polym. Sci.* **1991**, *43*, 993.

47. Hsieh, K. H.; Chiang, Y. C.; Chern, Y. C.; Chiu, W. Y.; Ma C. C. *Angew. Chem.* **1991**, *193*, 89.

48. Pater, R. H. *Polym. Eng. and Sci.* **1991**, *31*, 20.

49. McDonel, E. T.; Baranwal, K. C.; Andries, J. C. In *Polymer Blends*; Paul, D. R.; Newman, S., Eds.; Academic: New York, 1978; Vol. 2.

50. Bae, Y. H.; Okano, T.; Ebert, C.; Huber, S.; Dave, S.; Kim, S. W. *J. Controll. Rel.* **1991**, *16*, 189.

51. Katono, H.; Sanui, K.; Ogata, N.; Okano, T.; Sakurai, Y. *Polym. J.* **1991**, *23*, 1179.

52. Desai, N. P.; Hubbell, J. A. *Macromolecules* **1992**, *25*, 226.

53. Solt, G. S. British Patent 728 508 1955.

54. Kolarz, B. N. *J. Polym. Sci., Symp. No. 47* **1974**, 197.

55. Trochimuczuk, W. presented at the IUPAC sponsored conference, Modification of Polymers, Bratislava, Czechslovakia July 1979.

56. Barrett, J. H.; Clemens, D. H. U. S. Patent 3 966 489, 1976.

57. Hatch, M. J. U. S. Patent 3 957 698, 1976.

58. Sederel, W. L.; DeJong, G. J. *J. Appl. Polym. Sci.* **1973**, *17*, 2835.

59. Grimmett, M. R. In *Adv. Heterocyc. Chem.*; Katritzky, A. R.; Boulton, A. J., Eds.; Academic: New York, 1980; Vol. 27, p 270.

60. Chen, W.; Boven, G.; Challa, G. *Macromolecules* **1991**, *24*, 3982.

61. van de Grampel, H. T.; Tan, Y. Y.; Challa, G. *Macromolecules* **1992**, *25*, 1041.

62. So, Y. *Macromolecules* **1992**, *25*, 516.

63. Brock, T.; Sherrington, D. C.; Tang, H. G. *Polymer* **1991**, *32*, 353.

64. Dambatta, B. B.; Ebdon, J. R.; Huckerly, T. N. *Eur. Polym. J.* **1984**, *20*, 645.

65. Bamford, C. H.; Schofield, E. *Polymer* **1981**, *22*, 1227.

66. Alexandratos, S. D.; Strand, M. A. *Macromolecules* **1986**, *19*, 273.

67. Gozdz, A. S. *Makromol. Chem., Rapid Commun.* **1981**, *2*, 443.

68. De Loecker, W.; Smets, G. *J. Polym. Sci.* **1959**, *40*, 203.

69. Lee, J. Y.; Painter, P. C.; Coleman, M. M. *Macromolecules* **1988**, *21*, 954.

70. Davankov, V. A.; Rogozhin, S. V.; Tsyurupa, M. P. In *Ion Exchange and Solvent Extraction*; Marinsky, J. A.; Marcus, Y., Eds.; Marcel Dekker: New York, 1977; Vol. 7, Chapter 2.

71. Shea, K. J.; Sasaki, D. Y. *J. Am. Chem. Soc.* **1989**, *111*, 3442.

72. Hammett, L. P. *Physical Organic Chemistry*, 2nd ed; McGraw-Hill: New York, 1970.

73. Shriver, D. F.; Atkins, P. W.; Langford, C. H. *Inorganic Chemistry*; Freeman: New York, 1990; Chapter 6.

74. Kotrly, S.; Sucha, L. *Handbook of Chemical Equilibria in Analytical Chemistry*; Ellis Horwood: Chichester, U. K., 1985.

75. Martell, A. E.; Sillin, L. G. *Stability Constants of Metal-Ion Complexes*, 2nd ed; The Chemical Society: London, 1964.

76. Fujata, H.; Yanagida, S.; Okahara, M. *Anal. Chem.* **1980**, *52*, 869.

77. Laidler, K. J. *Physical Chemistry with Biological Application*; Benjamin/Cummings: Menlo Park, 1978.

78. Connors, K. A. *Binding Constants*; Wiley: New York, 1987.

79. Chang, W. K. Ph. D. Dissertation, University of Tennessee, Aug. 1992.

80. Beauvais, Robert, unpublished observations.

81. Deranleau, D. A. *J. Am. Chem. Soc.* **1969**, *91*, 4044.

APPENDIX

An expression for quantitatively describing the strength of the binding of ligands and substrates has been employed. It is important to have an equation relating the amount of a substance complexed, or adsorbed, to the concentration of the substance present in the solution[77]. Such equations apply at a fixed temperature and are known as adsorption isotherms. The simplest adsorption isotherm was first obtained by the American physical chemist Irving Langmuir[78] and is shown in Equation 1. The basis of the derivation of the Langmuir

$$y = \frac{ax}{b + x} \qquad (1)$$

adsorption isotherm is that all parts of the surface behave the same in adsortion and that binding occurs in a 1:1 ratio. Connors[78] described several graphical representations of the isotherm including the direct plot, semi-logarithmic plot, log-log plot, double-reciprocal plot, and *y*-reciprocal plot[78].

In the molecular and ionic recognition studies previously described, a broad range of substrate concentrations is used to give a well-defined isotherm. The number of milliequivalents of polymer ligands was equal to one in all studies. After the system reached equilibrium, the final concentration of the substrate in the solution was determined.

Assume the following equilibria:

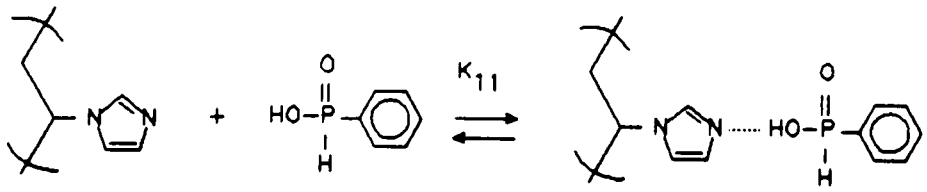


Figure A1. VIm IPN Complexation of PPA.

The fraction of the ligands in the form of LS is described as f_{11} as shown in Equation 2, and K_{11} is defined in Equation 3. The subscript "11" refers to a one to one binding.

$$f_{11} = \frac{[LS]}{L_{total}} \tag{2}$$

$$K_{11} = \frac{[LS]}{[L]\ [S]} \tag{3}$$

Therefore,

$$[LS] = K_{11}\ [L]\ [S] \tag{4}$$

Substituting Equation 4 into Equation 2 and realizing that L_{total}= [L] + [L S],

$$f_{11} = \frac{K_{11}\,[L]\,[S]}{[L] + [LS]} \tag{5}$$

$$f_{11} = \frac{K_{11}\,[L]\,[S]}{[L] + K_{11}\,[L]\,[S]} \tag{6}$$

$$f_{11} = \frac{K_{11}\,[S]}{1 + K_{11}\,[S]} \tag{7}$$

$$\frac{[LS]}{L_{total}} = \frac{K_{11}\,[S]}{1 + K_{11}\,[S]} \tag{8}$$

The variables r and c are defined in Equations 9 and 10.

$$r = [LS] = \frac{\textit{mequiv. of PPA bound}}{\textit{grams of dry resin}} \tag{9}$$

$$c = [S] = \frac{\textit{mequiv. of free PPA}}{\textit{ml of solution}} \tag{10}$$

L_{total} is defined as the saturation capacity, S_t. After making these substitutions,

$$\frac{r}{S_t} = \frac{K_{11}\,c}{1 + K_{11}\,c} \tag{11}$$

If one takes the reciprocal of Equation 11,

$$\frac{S_t}{r} = \frac{1 + K_{11}\,c}{K_{11}\,c} \tag{12}$$

divides by S_t and separates the right side of the equation,

$$\frac{1}{r} = \frac{1}{S_t} + \frac{1}{K_{11}\, c\, S_t} \tag{13}$$

and multiply by c,

$$\frac{c}{r} = \frac{1}{S_t}\, c + \frac{1}{K_{11}\, S_t} \tag{14}$$

the result is the y-reciprocal form of the Langmuir isotherm as described by Connors[78].

To determine the binding constant, the experimental values of r and c are plotted as shown in Figure A2. The saturation capacity, S_t, of the substrate onto

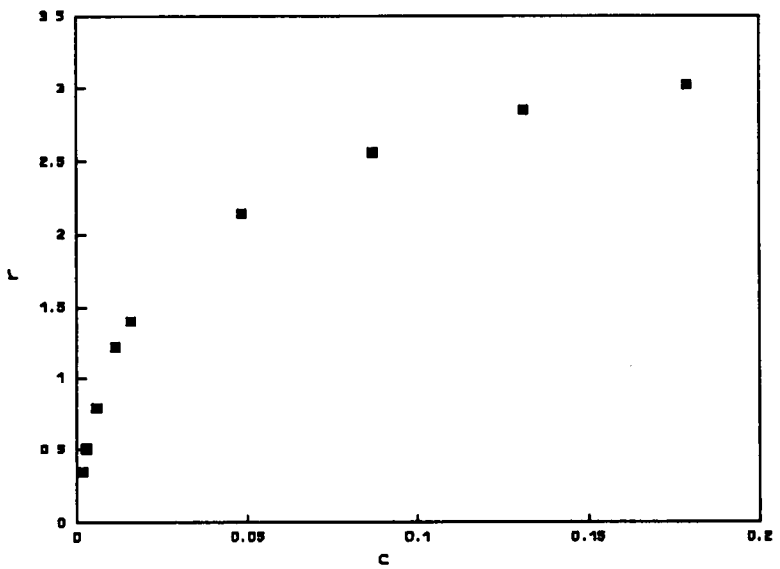


Figure A2. Adsorption Isotherm of VIm IPN with PPA.

the polymer is determined by the value of r at the point where the adsorption isotherm levels off. Connors[78] denotes this curve as the direct plot and states that it is often called the binding curve.

The complexation data, r and c, are then fitted to a modified Langmuir isotherm equation[79] as shown below with a, b, and k as empirical parameters.

$$r = \frac{a\,c^{k}}{b + c^{k}} \tag{15}$$

When the exponent k is equal to 1.0, the equation becomes the Langmuir adsorption isotherm equation shown in equation 1. In the work described in this thesis, the exponent k was in a range of 0.8 to 1.2. Subsequent work has shown that when k=1, the K_{11} does not depend heavily on the value of k=0.8 to 1.2[80]. The experimental equation is used instead of the regular Langmuir isotherm equation because it is a better fit to the experimental data (correlation coefficients at least 0.99). The binding constant K_{11} was then calculated from the y-reciprocal form of the Langmuir equation (Equation 14). Seven evenly spaced[78] points between 20% and 80% of the saturation capacity are utilized as shown in Figure A3. The range of 20% to 80% was recommended by Deranleau[81]. The binding constant is then calculated from the *y*-reciprocal plot as shown in Equation 16.

$$K_{11} = \frac{slope}{intercept} \tag{16}$$

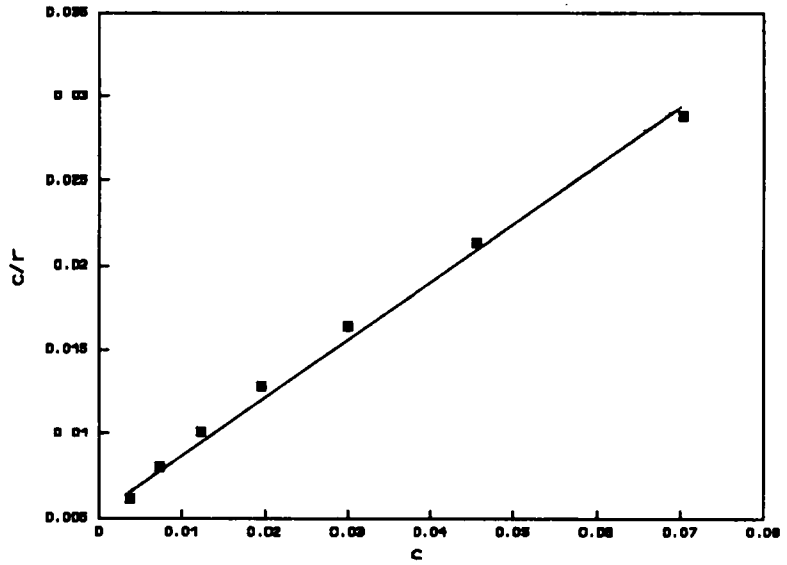


Figure A3. *y*-Reciprocal Plot of VIm IPN with PPA.

VITA

Corinne Grady Ciaccio was born in Corinth, Mississippi on January 15, 1968. She attended elementary schools in that city and graduated from Corinth High School in May 1986. Corinne graduated with honors from Millsaps College in May 1990 with a Bachelor of Science degree in Chemistry. In July 1990, she accepted a teaching and research assistantship from the Chemistry Department at the University of Tennessee and began study toward the Master of Science degree in Polymer Chemistry under the guidance of Dr. Spiro D. Alexandratos. The degree was awarded in December 1992.

The author is a member of the American Chemical Society and Phi Beta Kappa. She is employed by Millsaps College in Jackson, Mississippi.